

UNCLASSIFIED

AD NUMBER
ADB004290
NEW LIMITATION CHANGE
TO Approved for public release, distribution unlimited
FROM Distribution authorized to U.S. Gov't. agencies only; Test and Evaluation; 19 Dec 1974. Other requests shall be referred to Air Force Cambridge Research Lab., Attn: LY, Hanscom AFB, MA 01731.
AUTHORITY
Air Force Geophysics Lab ltr dtd 6 Nov 1980

THIS PAGE IS UNCLASSIFIED

AFCRL-TR-74-0627
AIR FORCE SURVEYS IN GEOPHYSICS, NO. 297



ADB004290

**Aircraft and Radar Weather Data Analysis
for PVM-5
AFCRL/Minuteman Report No. 1**

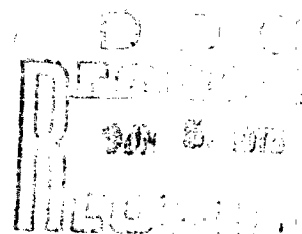
ARNOLD A. BARNES, Jr.
JAMES I. METCALF, 1 Lt, USAF
LOREN D. NELSON

23 December 1974

Distribution limited to U.S. Government agencies
only; (Test and Evaluation of Commercial Products
or Military Hardware); (19 December 1974). Other
requests for this document must be referred to
AFCRL (LY), Hanscom AFB, Massachusetts 01731

METEOROLOGY LABORATORY PROJECT 133B
AIR FORCE CAMBRIDGE RESEARCH LABORATORIES
HANSCOM AFB, MASSACHUSETTS 01731

AIR FORCE SYSTEMS COMMAND, USAF



Qualified requestors may obtain additional copies from the Defense Documentation Center. All others should apply to the National Technical Information Service.

Unclassified

REPORT DOCUMENTATION PAGE		READ INSTRUCTIONS BEFORE COMPLETING FORM
1. REPORT NUMBER AFCRL-TR-74-0627	2. GOVT ACCESSION NO.	3. RECIPIENT'S CATALOG NUMBER
4. TITLE (and Subtitle) AIRCRAFT AND RADAR WEATHER DATA ANALYSIS FOR PVM-5 AFCRL/MINUTEMAN REPORT NO. 1		5. TYPE OF REPORT & PERIOD COVERED Scientific. Interim.
		6. PERFORMING ORG. REPORT NUMBER AFSG No. 297
7. AUTHOR(s) Arnold A. Barnes, Jr. James I. Metcalf, 1 Lt, USAF Loren D. Nelson		8. CONTRACT OR GRANT NUMBER(s)
9. PERFORMING ORGANIZATION NAME AND ADDRESS Air Force Cambridge Research Laboratories (LY) Hanscom AFB Massachusetts 01731		10. PROGRAM ELEMENT PROJECT, TASK AREA & WORK UNIT NUMBERS 133B0001
11. CONTROLLING OFFICE NAME AND ADDRESS Air Force Cambridge Research Laboratories (LY) Hanscom AFB Massachusetts 01731		12. REPORT DATE 23 December 1974
		13. NUMBER OF PAGES 47
14. MONITORING AGENCY NAME & ADDRESS (if different from Controlling Office)		15. SECURITY CLASS. (of this report) Unclassified
		15a. DECLASSIFICATION/DOWNGRADING SCHEDULE
16. DISTRIBUTION STATEMENT (of this Report) Distribution limited to U.S. Government agencies only: (Test and Evaluation of Commercial Products or Military Hardware); (19 December 1974). Other requests for this document must be referred to AFCRL (LY), Hanscom AFB, Massachusetts 01731.		
17. DISTRIBUTION STATEMENT (of the abstract entered in Block 20, if different from Report)		
18. SUPPLEMENTARY NOTES *Bureau of Reclamation, Denver, Colorado		
19. KEY WORDS (Continue on reverse side if necessary and identify by block number) Radar weather measurement Tropical cirrus cloud Z-M equations Aircraft weather measurement Water content profiles		
20. ABSTRACT (Continue on reverse side if necessary and identify by block number) Aircraft and radar weather data recorded for support of the Minuteman PVM-5 test are presented. The link-offset mode was used successfully to obtain radar data for correlation with the aircraft data. The correlation data were quite good, and provided usable relations of reflectivity factor (Z) and water content (W) on five or nine passes. Application of these Z-W relations to the reflectivity data recorded along the re-entry trajectories provided estimates of the water content profile and the weather severity index (WSI) for each of the trajectories.		

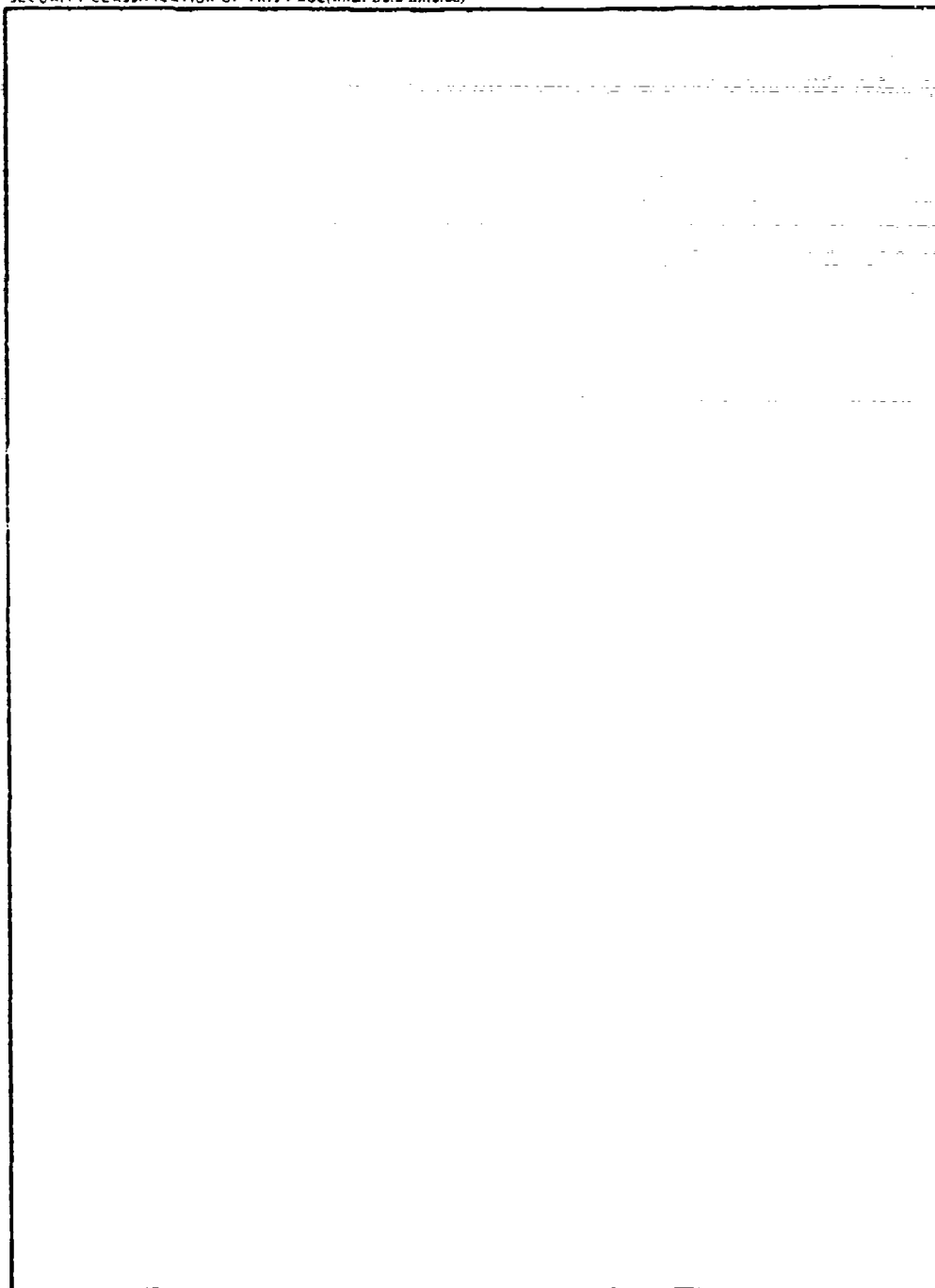
DD FORM 1 JAN 73 1473 EDITION OF 1 NOV 68 IS OBSOLETE

Unclassified

SECURITY CLASSIFICATION OF THIS PAGE (When Data Entered)

Unclassified

SECURITY CLASSIFICATION OF THIS PAGE(When Data Entered)



Unclassified

SECURITY CLASSIFICATION OF THIS PAGE(When Data Entered)

Preface

INTRODUCTION TO THE MINUTEMAN REPORT SERIES

AFCRL has supported the SAMSO Minuteman Natural Hazards Program since June 1973. This support has included technical assistance in defining meteorological objectives and experimental procedures, and analysis of aircraft and radar weather data obtained in conjunction with each mission. A major part of the latter function includes analysis of aircraft and radar data taken jointly to derive correlations of radar reflectivity factor Z and water content M.

Because of the number of missile tests in the program it seemed advisable to initiate a special sub-series of AFCRL Technical Reports devoted to the program. In addition, because of the desirability of presenting the results of the correlation data analysis in considerable detail, we intend to publish these results separately for days on which these data were recorded. The final reports for particular missions will only summarize the analytical results previously published, rather than including those results in detail.

Contents

1.	INTRODUCTION	9
2.	AIRCRAFT DATA	10
3.	RADAR DATA	12
4.	CORRELATION DATA ANALYSIS	15
	4.1 Pass 1	16
	4.2 Pass 2	19
	4.3 Pass 3	21
	4.4 Pass 4	24
	4.5 Pass 5	27
	4.6 Pass 6	29
	4.7 Pass 7	32
	4.8 Pass 8	34
	4.9 Pass 9	37
5.	INTERPRETATION OF THE RV TRAJECTORY RADAR DATA	39
6.	CONCLUSIONS	43
	REFERENCES	45
	SYMBOLS	47

Illustrations

1. Aircraft Flight Paths and RV Trajectories at Kwajalein	11
2. Reflectivity Profiles for PVM-5, RV 1 Trajectory	13
3. Reflectivity Profiles for PVM-5, RV 2 Trajectory	14
4. Reflectivity Profiles for PVM-5, RV 3 Trajectory	15
5. Water Content and Reflectivity Computed From Aircraft Data for Pass 1 at 12.9 km	17
6. Correlation of M_a and Z_a Data From Figure 5	17
7. Reflectivity Measured by Radar (lower) and Water Content Inferred From the Reflectivity (upper) for Pass 1	18
8. Correlation of M_a From Figure 5 and Z_r and From Figure 7	18
9. Water Content and Reflectivity Computed From Aircraft Data for Pass 2 at 12.1 km	19
10. Correlation of M_a and Z_a Data From Figure 9	20
11. Reflectivity Measured by Radar (lower) and Water Content Inferred From the Reflectivity (upper) for Pass 2	20
12. Correlation of M_a From Figure 9 and Z_r From Figure 11	21
13. Water Content and Reflectivity Computed From Aircraft Data for Pass 3 at 11.4 km	22
14. Correlation of M_a and Z_a Data From Figure 13	22
15. Reflectivity Measured by Radar (lower) and Water Content Inferred From the Reflectivity (upper) for Pass 3	23
16. Correlation of M_a From Figure 13 and Z_r From Figure 15	23
17. Water Content and Reflectivity Computed From Aircraft Data for Pass 4 at 10.4 km	24
18. Correlation of M_a and Z_a Data From Figure 17	25
19. Reflectivity Measured by Radar (lower) and Water Content Inferred From the Reflectivity (upper) for Pass 4	26
20. Correlation of M_a From Figure 17 and Z_r From Figure 19	26
21. Water Content and Reflectivity Computed From Aircraft Data for Pass 5 at 9.7 km	27
22. Correlation of M_a and Z_a Data From Figure 21	28
23. Reflectivity Measured by Radar (lower) and Water Content Inferred From the Reflectivity (upper) for Pass 5	28
24. Correlation of M_a From Figure 21 and Z_r From Figure 23	29
25. Water Content and Reflectivity Computed From Aircraft Data for Pass 6 at 9.0 km	30
26. Correlation of M_a and Z_a Data From Figure 25	30
27. Reflectivity Measured by Radar (lower) and Water Content Inferred From the Reflectivity (upper) for Pass 6	31
28. Correlation of M_a From Figure 25 and Z_r From Figure 27	31

Illustrations

29.	Water Content and Reflectivity Computed From Aircraft Data for Pass 7 at 8.1 km	32
30.	Correlation of M_a and Z_a Data From Figure 29	33
31.	Reflectivity Measured by Radar (lower) and Water Content Inferred From the Reflectivity (upper) for Pass 7	33
32.	Correlation of M_a From Figure 29 and Z_r From Figure 31	34
33.	Water Content and Reflectivity Computed From Aircraft Data for Pass 8 at 7.3 km	35
34.	Correlation of M_a and Z_a Data From Figure 33	35
35.	Reflectivity Measured by Radar (lower) and Water Content Inferred From the Reflectivity (upper) for Pass 8	36
36.	Correlation of M_a From Figure 33 and Z_r From Figure 35	36
37.	Water Content and Reflectivity Computed From Aircraft Data for Pass 9 at 6.6 km	37
38.	Correlation of M_a and Z_a Data From Figure 37	38
39.	Reflectivity Measured by Radar (lower) and Water Content Inferred From the Reflectivity (upper) for Pass 9	38
40.	Correlation of M_a From Figure 37 and Z_r From Figure 39	39
41.	Composite of Z-M Equations Derived From PVM-5 Correlation Data	40
42.	Water Content Profile on PVM-5, RV 1 Trajectory	42
43.	Water Content Profile on PVM-5, RV 2 Trajectory	42
44.	Water Content Profile on PVM-5, RV 3 Trajectory	43

Tables

1.	$Z_r - M_a$ Relations, April 1974	41
----	-----------------------------------	----

Aircraft and Radar Weather Data Analysis for PVM-5 AFCRL/Minuteman Report No. 1

I. INTRODUCTION

This report presents the derivation of water content profiles on the PVM-5 re-entry trajectories. PVM-5 was the first mission in which the re-entry vehicles were intentionally flown through clouds. Weather data were obtained jointly by the WE-57F weather reconnaissance aircraft and by ALCOR, a tracking radar at Roi-Namur Island. Specialized data processing and analysis techniques were developed for this purpose. These were adaptations and refinements of techniques developed by AFCRL for the SAMSO/ABRES program field work at Wallops Island, Virginia.^{1,2,3} A brief description of the experiment was presented by Barnes et al.⁴

(Received for publication 20 December 1974)

1. Plank, V. G. (1974a) A summary of the radar equations and measurement techniques used in the SAMS rain erosion program at Wallops Island, Virginia. AFCRL-TR-0053, Air Force Cambridge Research Laboratories, Hanscom AFB, Mass.
2. Plank, V. G. (1974b) Hydrometeor parameters determined from the radar data of the SAMS rain erosion program. AFCRL-TR-74-0249, Air Force Cambridge Research Laboratories, Hanscom AFB, Mass.
3. Plank, V. G. (1974c) Liquid-water content and hydrometeor size-distribution information for the SAMS missile flights of the 1971-1972 season at Wallops Island, Virginia. AFCRL-TR-74-0296, Air Force Cambridge Research Laboratories, Hanscom AFB, Mass.
4. Barnes, A. A., Jr., Nelson, I. D., and Metcalf, J. I. (1974) Weather Documentation at Kwajalein Missile Range. 6th Conf. Aerosp. and Aeronaut. Meteor., Amer. Meteor. Soc. pp 66-69; AFCRL-TR-74-0430, Air Force Cambridge Research Laboratories, Hanscom AFB, Mass.

Radar weather data were recorded along the re-entry trajectories in a sequence of scans immediately after vehicle impact. The radar reflectivity factor Z is equal to the sixth moment of the particle size spectrum, and thus is not a direct measure of the water content M , which is proportional to the third moment of the size spectrum, or the volume. Because the relation between Z and M depends on the distribution of particle sizes within each cloud, correlations had to be obtained close to the time of the mission in order to interpret the reflectivity data on the trajectories. The Z - M relations were derived by correlation of radar and aircraft measurements made at several different altitudes within approximately two hours of re-entry.

2. AIRCRAFT DATA

Two WB-57F weather reconnaissance aircraft, operated by the 58th Weather Reconnaissance Squadron at Kirtland AFB, were used in this program. The principal cloud sensors were a formvar replicator built by Meteorology Research, Inc. (MRI), Altadena, Calif., and three particle detectors built by Particle Measuring Systems, Inc. (PMS), Boulder, Colorado.⁵ The three detectors measured particle sizes in the ranges 2 to 30 μ (axially scattering probe), 20 to 300 μ (optical array cloud droplet probe), and 200 to 3000 μ (optical array precipitation probe). The replicator film provides a qualitative determination of the type of particles observed or, for ice crystals, the principal crystal habit. The sensors were operated by MRI, who also computed water content (M_a , gm m^{-3}), and reflectivity factor (Z_a , $\text{mm}^6 \text{m}^{-3}$) from the size spectrum data, following the technique of Heymsfield and Knollenberg.⁶ The subscript "a" refers to the aircraft data. For the PVM-5 mission, MRI found a predominance of plate crystals on the replicator films, and assumed 100 percent plate crystals in computing M_a and Z_a . These data were supplied as 1-sec averages, but we found it necessary to smooth the data with a 5-sec running mean to reduce noise characteristics before making the correlation with the radar data.

The reflectivity Z_a computed from the aircraft data cannot be identified precisely with that measured by the radar because of an uncertain calibration factor in the radar data processing. However, correlations of M_a and Z_a are useful in obtaining preliminary estimates of the Z - M equation and particularly in observing the variations of the Z - M equations on days when little or no radar data

5. Knollenberg, R. G. (1970) The optical array: An alternative to scattering or extinction for airborne particle size determination, J. Appl. Meteor. 9:86-103.

6. Heymsfield, A. J., and Knollenberg, R. G. (1972) Properties of cirrus generating cells. J. Atmos. Sci. 29:1358-1366.

are available. Aircraft data from different days have yielded Z-M equations differing by more than an order of magnitude in water content within the range of values of interest in these studies.

On the PVM-5 mission day, 5 April 1974, nine aircraft passes were made between 6.6 and 12.9 km in conjunction with the radar scanning described in Section 3. The flight paths, shown in Figure 1, were in the general area of the re-entry trajectories. The north and west headings were placed so as to bring the aircraft over Gellinam Island, where the Stanford Research Institute LIDAR was located. Further constraints on the location of the flight paths were that they not be radials to the radar and that the aircraft and the radar weather sampling gate not be at the same slant range, to avoid possible contamination of the radar data by backscatter from the aircraft in a side-lobe.

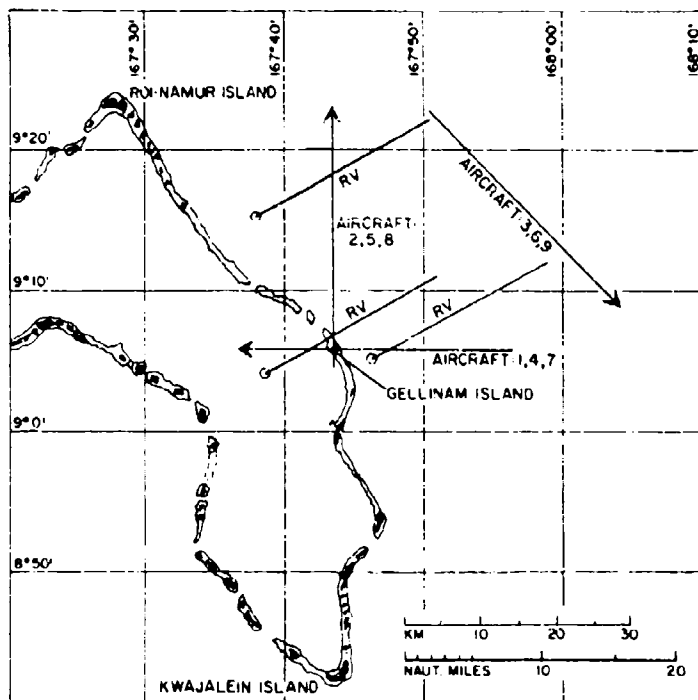


Figure 1. Aircraft Flight Paths and RV Trajectories at Kwajalein. Flight paths are numbered starting with the uppermost at 12.9 km. RV trajectories are indicated approximately from 15 km to the surface

The cloud probe malfunctioned during the mission, and MRI deleted these data from their computations. The resulting values of M_a and Z_a are based essentially on data from the precipitation probe, as the contribution from small particles, measured by the scattering probe, was very small. Our tentative conclusion is that the omission of the cloud probe data does not affect the results significantly, except at low values of M_a and Z_a , but we intend to resolve this problem by analysis of data from other days.

3. RADAR DATA

ALCOR, one of the Lincoln Laboratory radars at Kwajalein Missile Range, was used to record weather data at C-band (5.3 cm wavelength) in conjunction with the aircraft operations. The scanning involved a "link-offset" mode developed by AFCRL for use with this radar. The aircraft tracking data (from the MPS-36 radar at Kwajalein) were fed to the computer controlling ALCOR, and an adjustable offset distance (normally 3 km) was added so that the weather data were recorded ahead of the aircraft position along its path. A preliminary test in December 1973 using the TTR-4 radar operated by RCA at Kwajalein and one of the WE-57Ts had shown that the technique worked and would provide us with much better correlation data than the constant altitude radar scan method adapted from the Wallops Island program and used in support of PVM-3 and STM-8W. The link-offset mode was incorporated at KREMS and was successfully tested prior to PVM-5 using a C-54 supplied by KMR.

The ALCOR cross-section data from the radar tracking gate were recorded on the B-6 tape at the PRESS computer. The maximum cross-section in the four gates closest to the tracking point was sent from ALCOR to PRESS at a rate of 10 per sec (1/20 of the actual PRF) and averaged over 1-sec intervals. This averaging would be inadequate for a conventional pulsed weather radar, but the pulse compression applied to the frequency-modulated "chirp" radar pulse effectively smooths the noise normally encountered when using constant-frequency weather radars. The radar signal data were processed to yield values of reflectivity factor Z_r ($\text{mm}^6 \text{m}^{-3}$) for correlation with the aircraft data. The subscript "r" denotes the radar data. Because this computation involved an approximation for the equivalent pulse length for the chirp radar, the actual values of Z_r may be in error by a factor as large as 3 or 4. We are currently working on this problem, so as to specify Z_r precisely and be able to compare these values with Z_a computed from the aircraft data.

Radar weather data were taken along each of the re-entry trajectories immediately following vehicle impact. These were recorded both on the PRESS B-6 tape,

in the manner described above, and on ALCOR data tapes. The ALCOR tapes contain cross-section values at 170 range gates spaced across a 2.5-km interval around the tracking point which is located between gates 52 and 53. These provide a quasi-cross-sectional view of the weather in the vicinity of the trajectories, in addition to providing a comparison with the reflectivity values computed from the B-6 data. Reflectivity profiles computed from the B-6 data are shown in Figures 2, 3, and 4 for RV's 1, 2, and 3*. The sequence of scans on each trajectory provides a measure of the time variability of the reflectivity, and thus allows an evaluation of the accuracy of the profile actually encountered by the RV's. The interpretation of these profiles in terms of water content is described in the following sections.

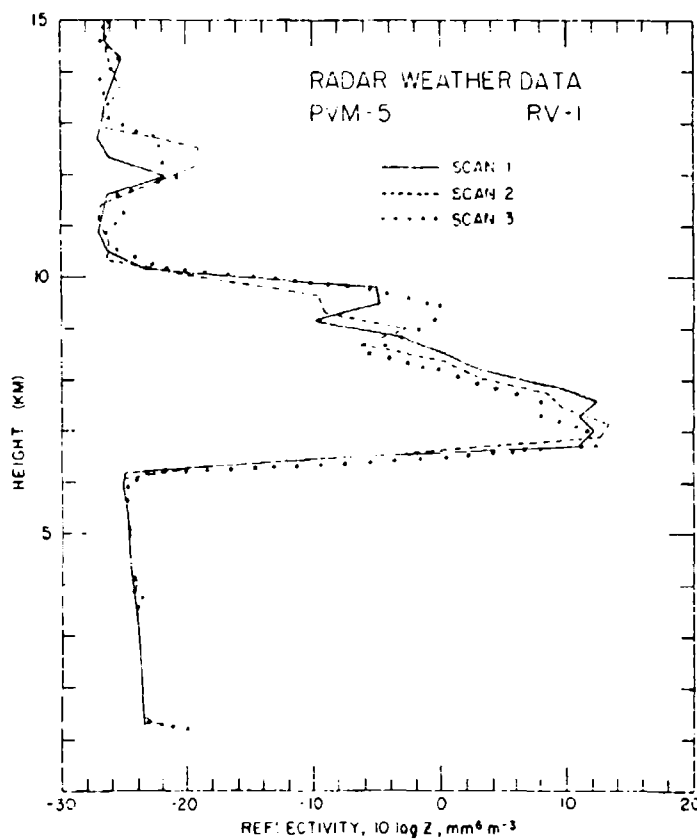


Figure 2. Reflectivity Profiles for PVM-5, RV 1 Trajectory. Three scans were taken, from 20 km to 1 km, starting at 0155:27, 0200:05, and 0204:34 GMT

* RV numbers denote the order of deployment, and have been corrected from the erroneous designations used in the draft of this report (29 May 1974) and in correspondence dated prior to 4 November 1974.

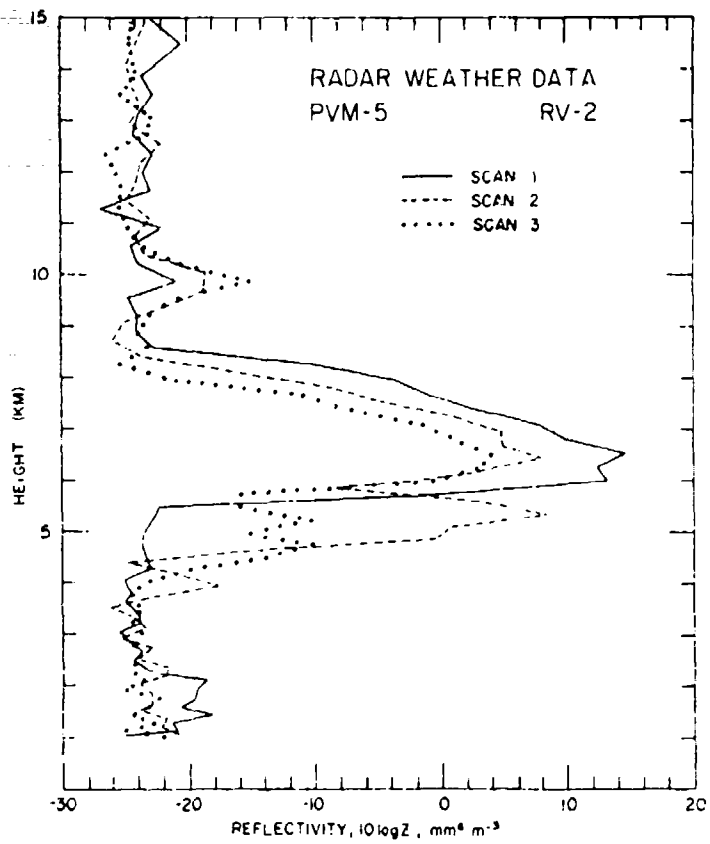


Figure 3. Reflectivity Profiles for PVM-5, RV 2 Trajectory. Three scans were taken, from 20 km to 1 km, starting at 0156:42, 0201:25, and 0205:53 GMT

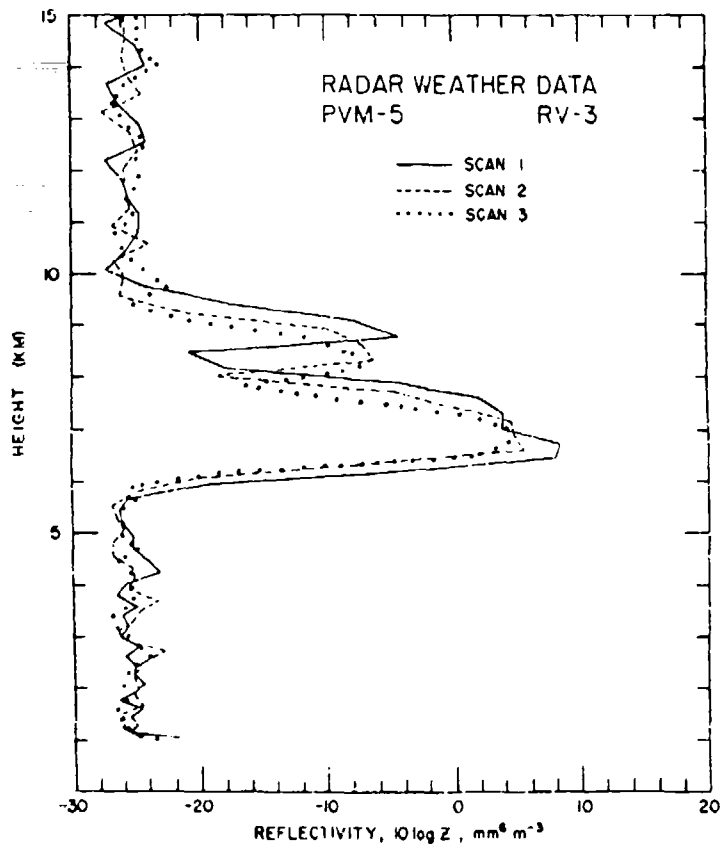


Figure 4. Reflectivity Profiles for PVM-5, RV 3 Trajectory. Three scans were taken from 20 km to 1 km, starting at 0154:03, 0158:45, and 0203:14 GMT

4 CORRELATION DATA ANALYSIS

Correlation of the aircraft and radar data was accomplished for each of the nine aircraft passes. While the offset distance was held constant, the offset time varied inversely with the aircraft speed, which was generally about 100 m sec^{-1} but lower at low altitude. The radar data from each pass were delayed in time relative to the aircraft data so as to maximize the correlation of $\log Z_a$ and $\log Z_r$. A correlation line was then computed for $\log M_a$ and $\log Z_r$ in the form

$$M_a = A Z_r^B,$$

or

$$\log M_a = \log A + B \log Z_r,$$

where M_a is measured in gm m^{-3} and Z_r in $\text{mm}^6 \text{m}^{-3}$. This relation was applied to the individual values of Z_r to obtain values of water content, designated M_r , for comparison with M_a derived from the aircraft data. Data and analysis for each of the nine passes are presented as follows (all plotted in logarithmic coordinates):

1. M_a and Z_a computed from the aircraft particle size spectrum data,
2. Correlation of M_a and Z_a ,
3. Z_r measured by radar and M_r inferred from radar data,
4. Correlation of M_a and Z_r .

4.1 Pass 1

This pass was made on a westerly heading at a mean altitude of 12.9 km determined by ALCOR, or an aircraft pressure altitude of 40,000 ft. The values of M_a and Z_a (Figure 5) are generally small, but they do fit onto a straight line with very little spread (Figure 6). The Z-M relation derived from the aircraft data seems fairly reasonable, although the coefficient 0.0051 is somewhat smaller than we would expect at this altitude. The values of Z_r (Figure 7) are close to the radar noise level, with very little variation along the scan. The variation of M_r is even less. The reason for this can be seen in Figure 8, where the tight grouping of the data yields an unreasonable Z-M relationship. We did not use this Z-M equation in our analysis of the trajectory reflectivity data.

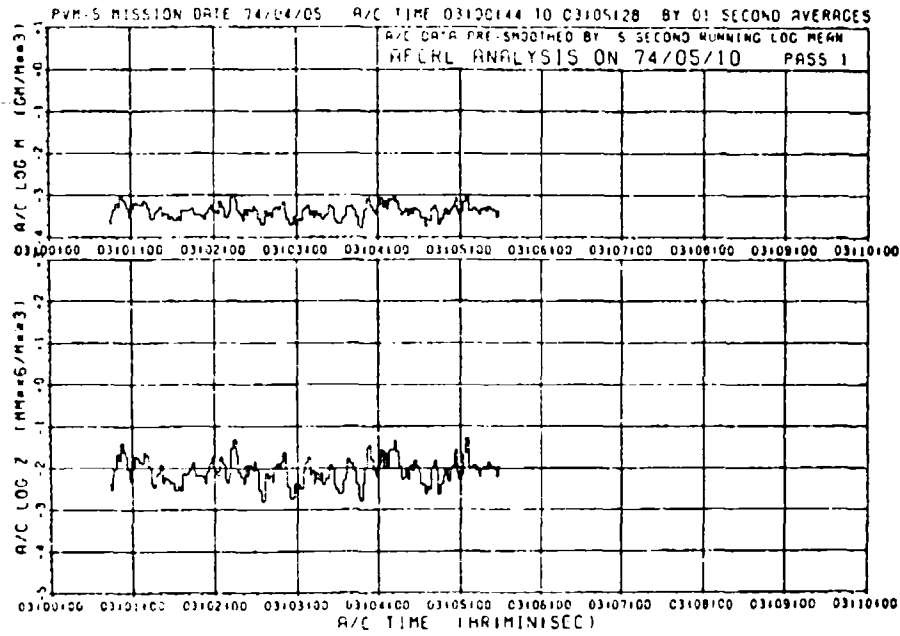


Figure 5. Water Content and Reflectivity Computed From Aircraft Data for Pass 1 at 12.9 km

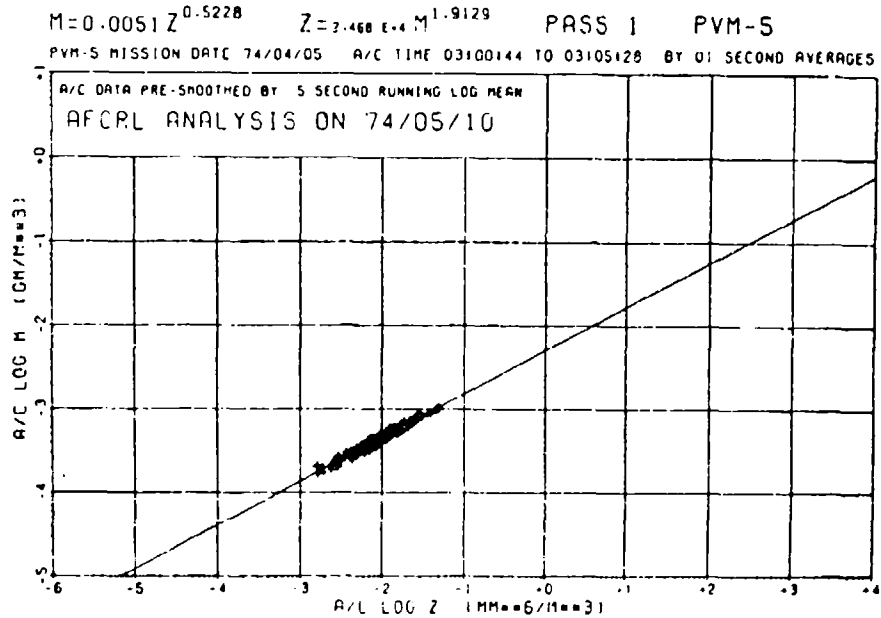


Figure 6. Correlation of M_a and Z_a From Figure 5

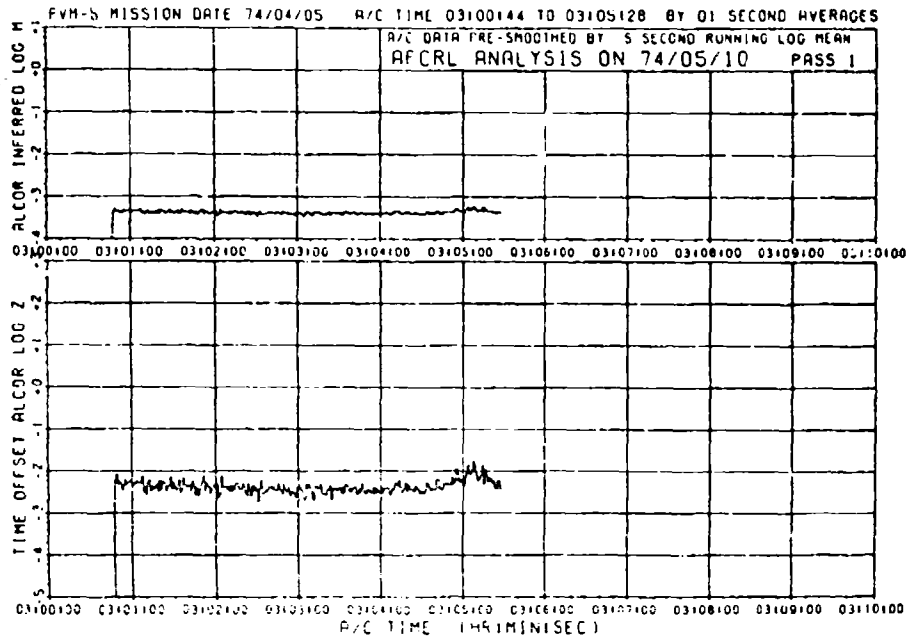


Figure 7. Reflectivity Measured by Radar (lower) and Water Content Inferred From the Reflectivity (upper) for Pass 1

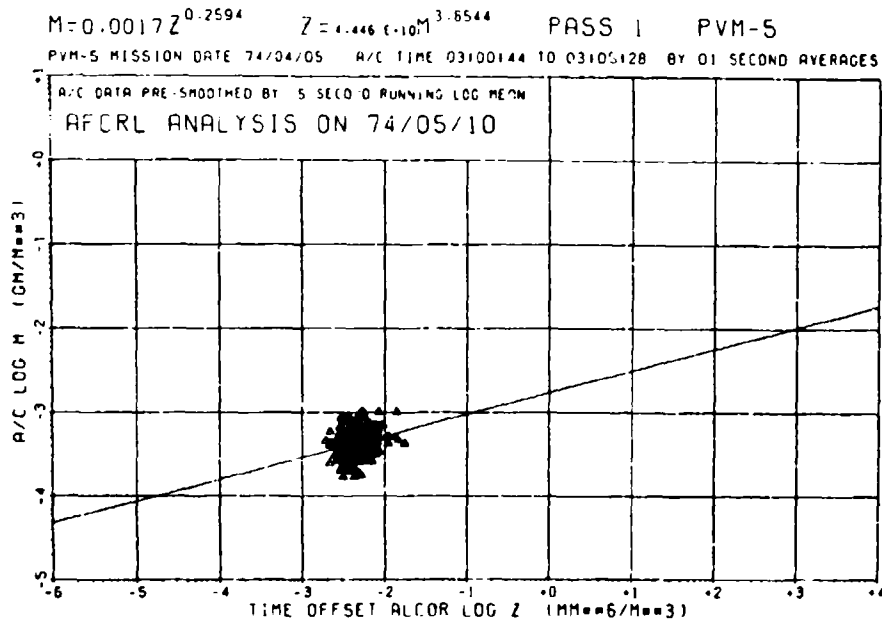


Figure 8. Correlation of M_a From Figure 5 and Z_r From Figure 7

4.2 Pass 2

This pass was made on a northerly heading at a mean radar height of 12.1 km, or 37,500 ft pressure altitude. The aircraft data (Figure 9) show maximum M_a values above 0.02 gm m^{-3} and maximum Z_a above $1.0 \text{ mm}^6 \text{ m}^{-3}$. Figure 10 shows that there was good spread in the data, but the correlation line seems too steep. We feel that the steepness is, to a minor extent, due to the absence of the cloud probe data, and that there is hope of obtaining the appropriate corrections by careful analysis of data collected on other days. The radar reflectivity data (Figure 11) show striking similarity to the Z_a values in Figure 9. Figure 12 shows the Z-M equation derived from this pass. This relation seems reasonable, although it is somewhat steep. We applied this relation to the uppermost part of the clouds.

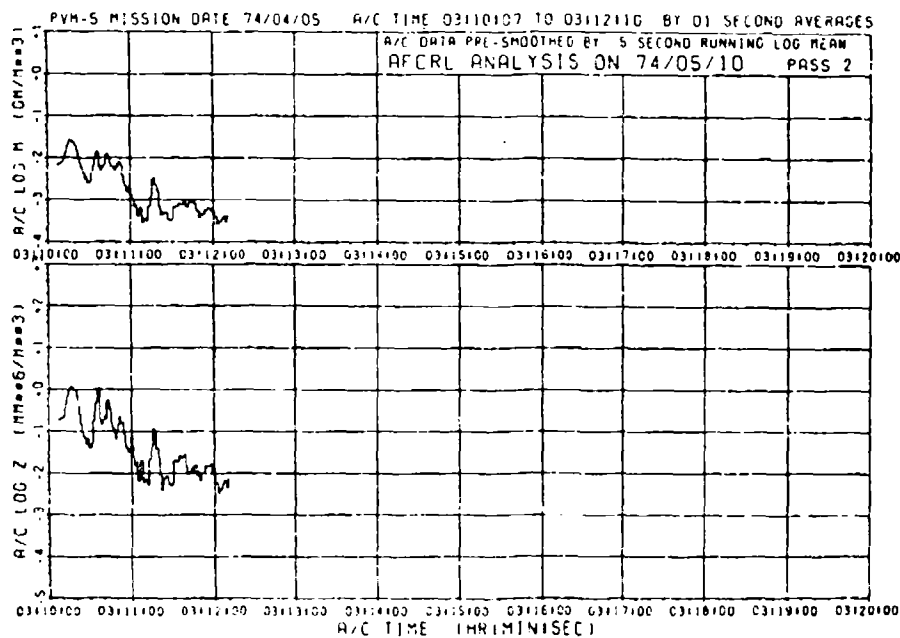


Figure 9. Water Content and Reflectivity Computed From Aircraft Data for Pass 2 at 12.1 km

$M = 0.0241 Z^{0.8146}$ $Z = 9.752 E-11 M^{1.2276}$ PASS 2 PVM-5
 PVM-5 MISSION DATE 74/04/05 A/C TIME 03110107 TO 03112110 BY 01 SECOND AVERAGES

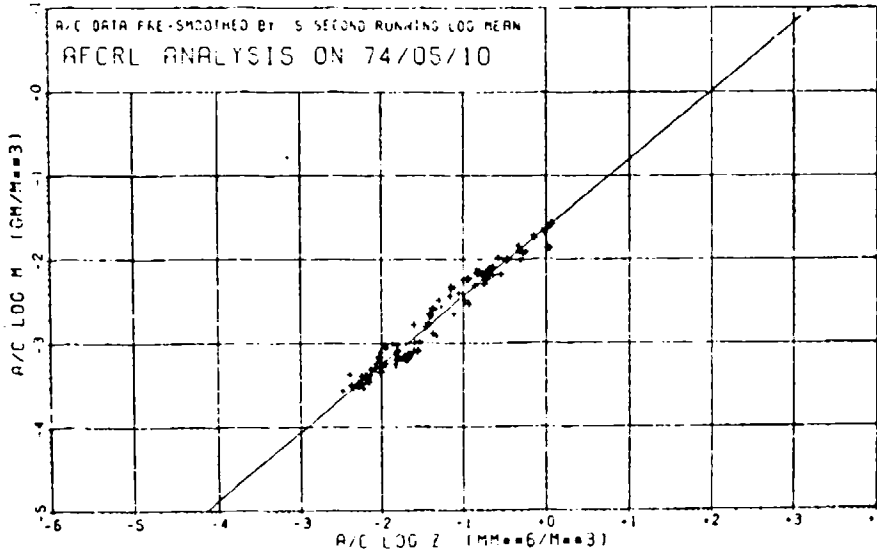


Figure 10. Correlation of M_a and Z_a Data From Figure 9

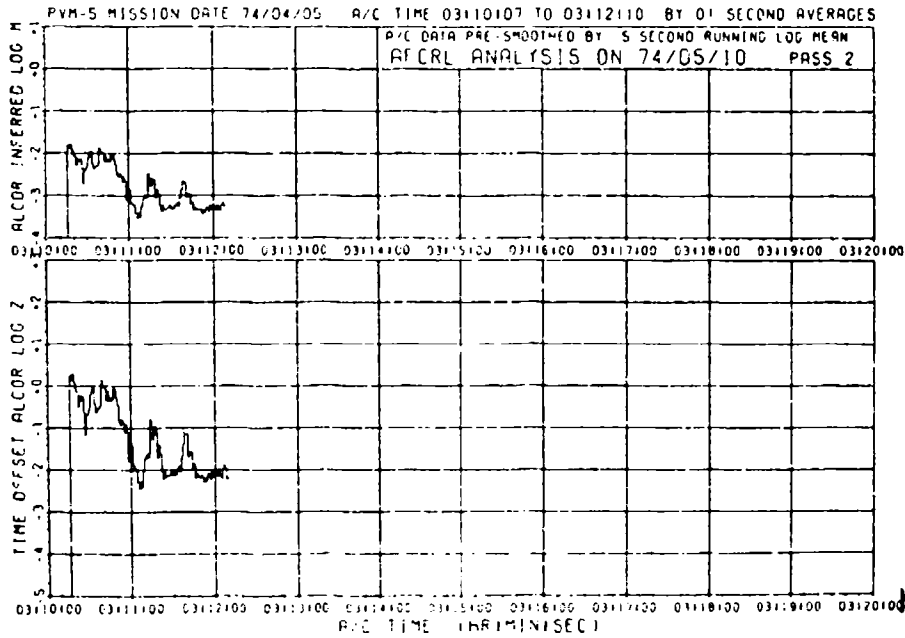


Figure 11. Reflectivity Measured by Radar (lower) and Water Content Inferred From the Reflectivity (upper) for Pass 2

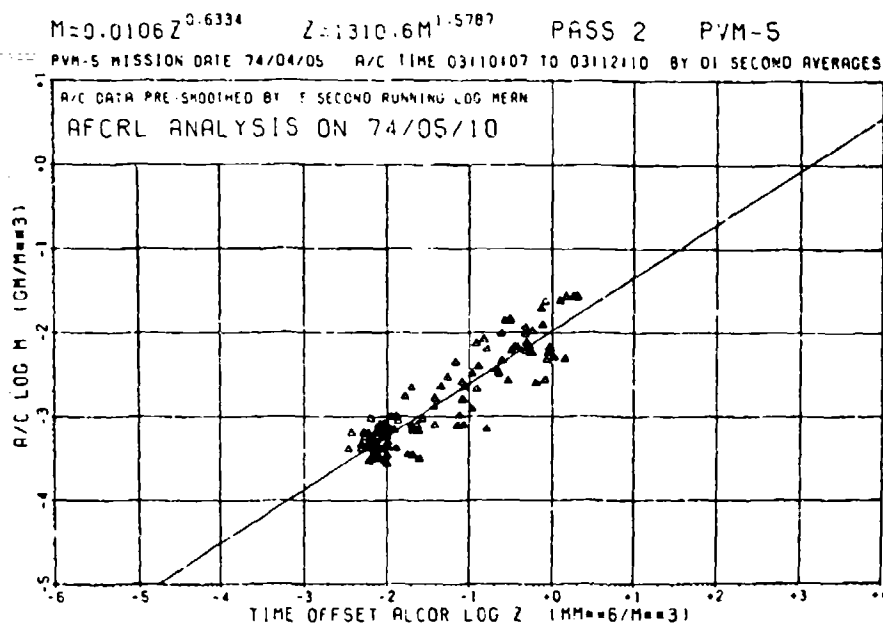


Figure 12. Correlation of M_a From Figure 9 and Z_r From Figure 11

4.3 Pass 3

The third pass was through thin clouds, on a 135° heading. The radar gave a mean height of 11.4 km, while the aircraft pressure altitude was 35,000 ft. Figures 13 and 14 both show that the aircraft did not go through heavy clouds. The radar data in Figure 15 indicate that the clouds were just above the radar noise level. This is dramatically evident in Figure 16, where all of the data points are in a small group. The Z-M relation therefore is of no significance and was not used in our analysis.

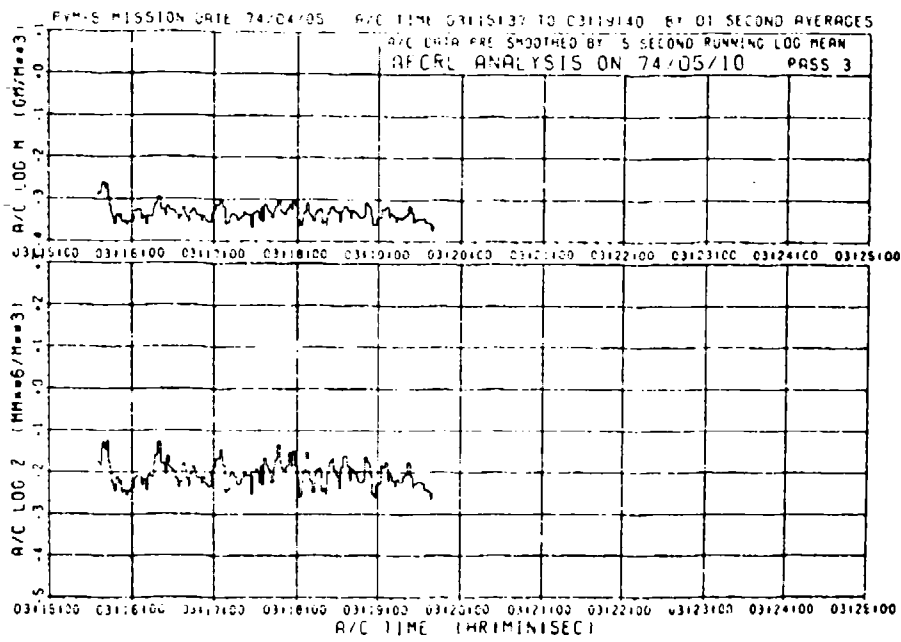


Figure 13. Water Content and Reflectivity Computed From Aircraft Data for Pass 3 at 11.4 km

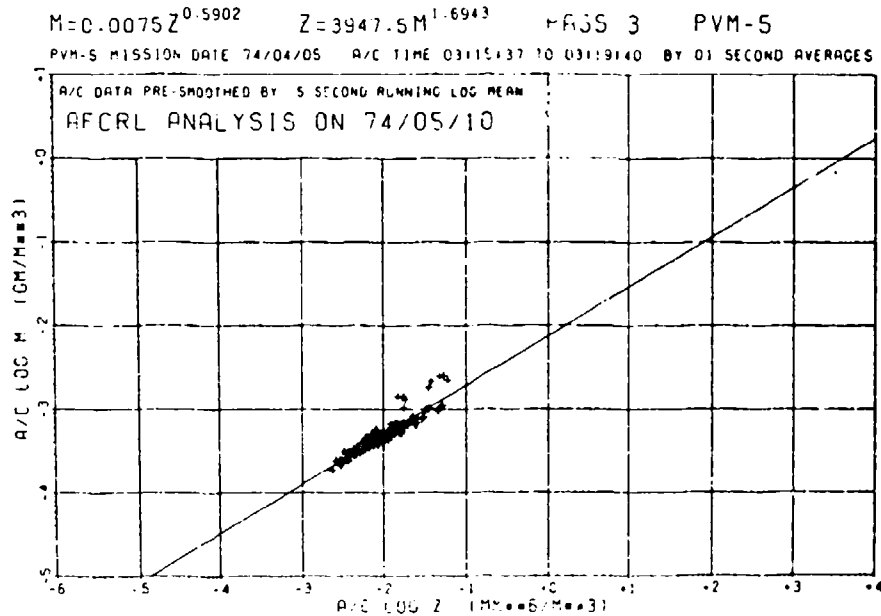


Figure 14. Correlation of M_a and Z_a Data From Figure 13

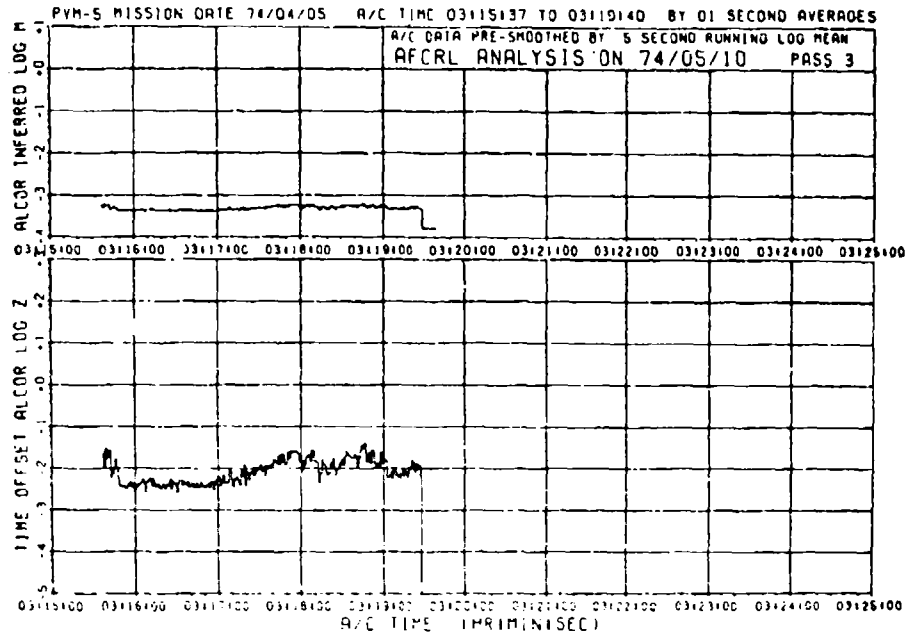


Figure 15. Reflectivity Measured by Radar (lower) and Water Content Inferred From the Reflectivity (upper) for Pass 3

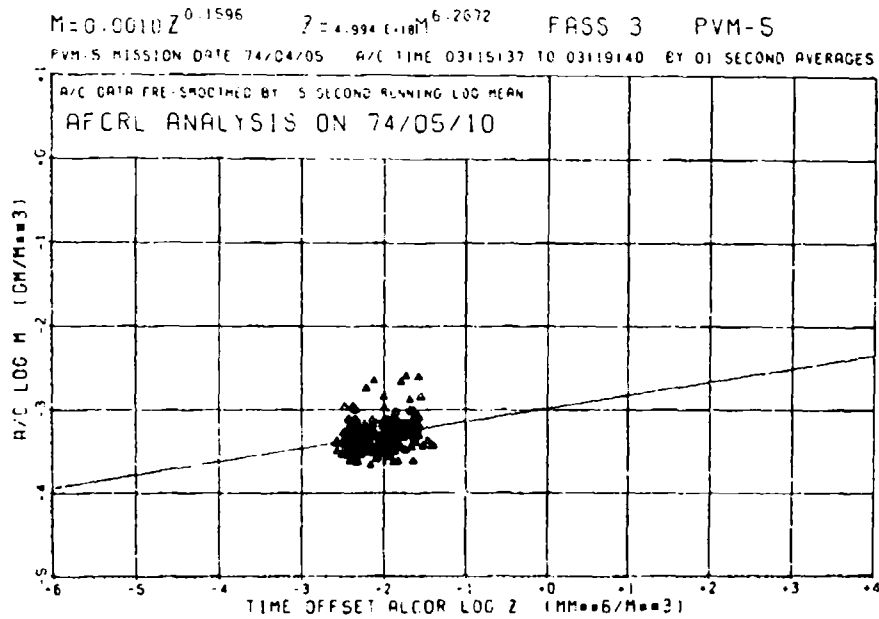


Figure 16. Correlation of M_a From Figure 13 and Z_r From Figure 15

4.4 Pass 4

This pass was flown at a pressure altitude of 32,500 ft, or a mean height of 10.4 km measured by ALCOR. This was the longest of the nine passes, lasting almost ten minutes. There was considerable evidence that there were some rather thick clouds over the lagoon so the east-to-west pass over Gellinam was extended. As can be seen in Figures 17 and 18, the aircraft M_a values cover three orders of magnitude and the Z_a values range over 4-1/2 orders of magnitude. These variations indicate that the flight penetrated some convective clouds. Note there is more spread of the points about the line in Figure 18 than in the analogous plot for any other pass except for Passes 5 and 6 which also passed through convective cells. This spread is due to the different particle size distributions in different parts of the same convective cell and at different times in the life cycle of the convective cells.

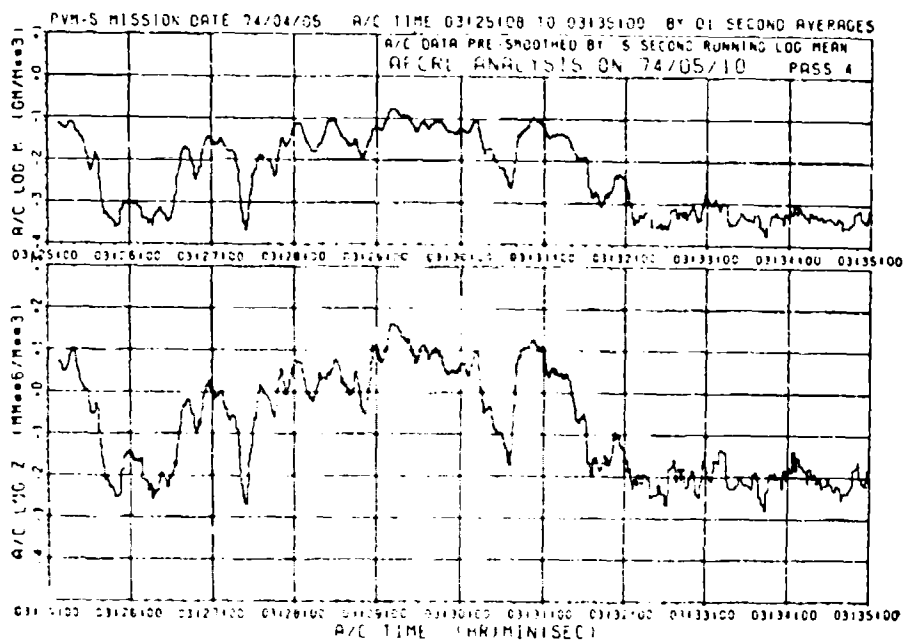


Figure 17. Water Content and Reflectivity Computed From Aircraft Data for Pass 4 at 10.4 km

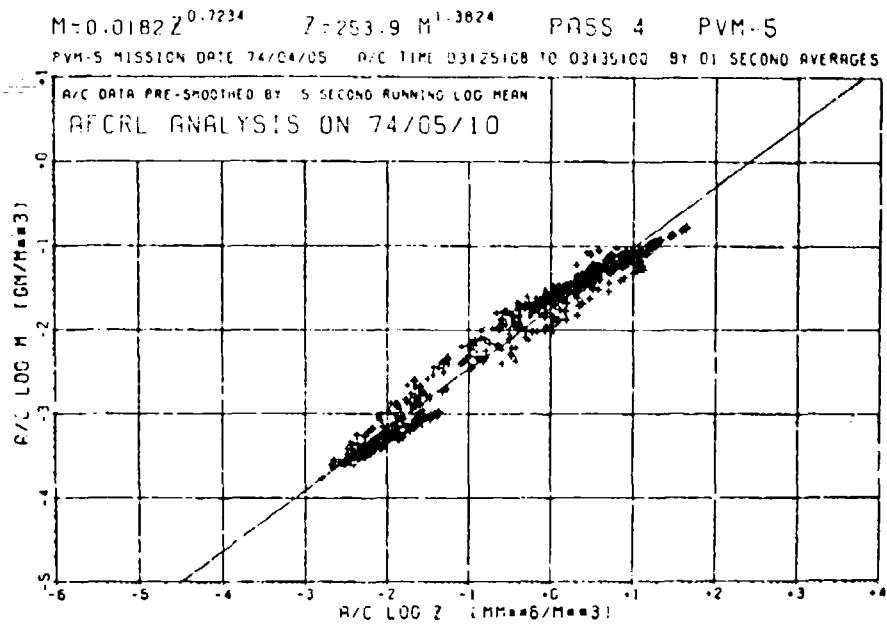


Figure 18. Correlation of M_a and Z_a Data From Figure 17

Because the aircraft and the radar tracking gate were at nearly the same range, the radar data from 0332:19 to 0334:31 were omitted from the analysis. The general features of Figures 17 and 19 are remarkably similar, but the deep minimum values obtained by the aircraft are not seen in the radar data. This is probably due to the difference in the sampling volumes of the radar and the aircraft. Figure 20 also shows the large spread we attribute to the variations of the size distributions. It should be noted that the spread is less at the upper end of the curve where the values are most reliable.

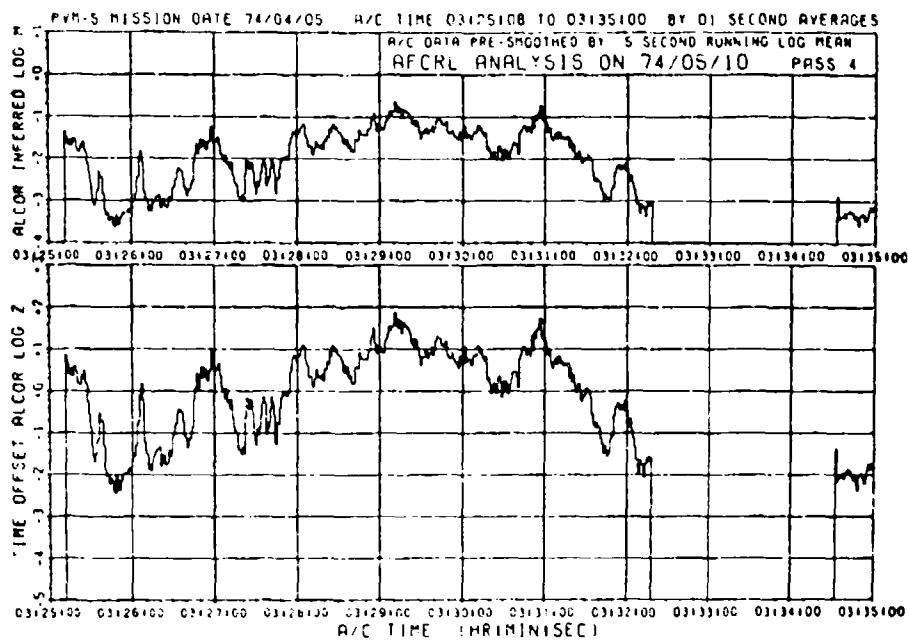


Figure 19. Reflectivity Measured by Radar (lower) and Water Content Inferred From the Reflectivity (upper) for Pass 4

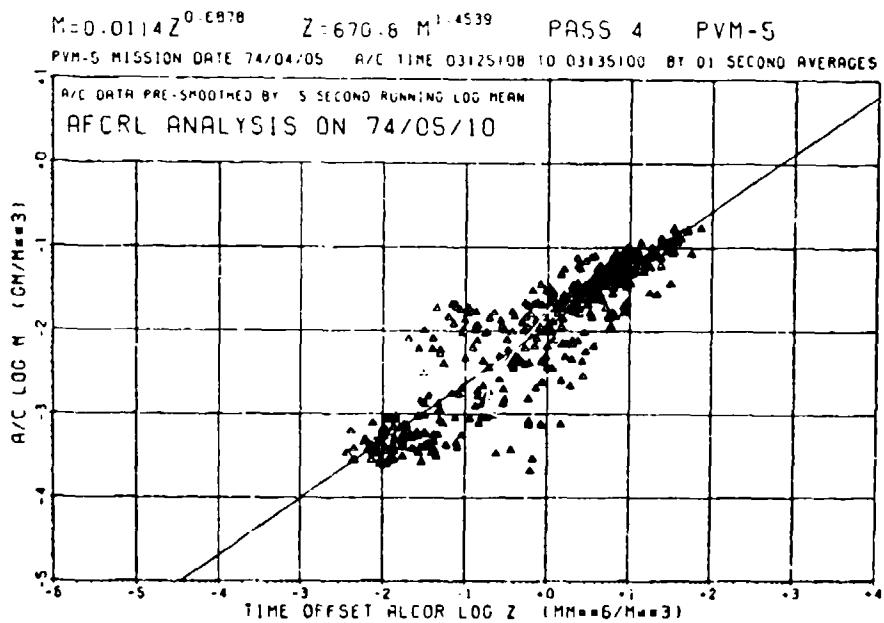


Figure 20. Correlation of M_a From Figure 17 and Z_r From Figure 19

4.5 Pass 5

This pass was made at 9.7 km, or 30,000 ft pressure altitude, on a northerly heading over Gellinam. The WB-57F was in and out of convective clouds, as can be seen from the aircraft data record of Figure 21 and from the spread of the data points about the correlation line in Figure 22. During the pass the ALCOR offset distance was changed temporarily. Because our analysis techniques do not compensate for such a variation we were forced to delete the radar data between 0344:51 and 0346:09 in Figure 23, most of which, fortunately, was in the region of low reflectivity. Thus only the higher values of Z_r and M_a went into the correlation shown in Figure 24. This Z-M relation falls close to those derived for Passes 2 and 4.

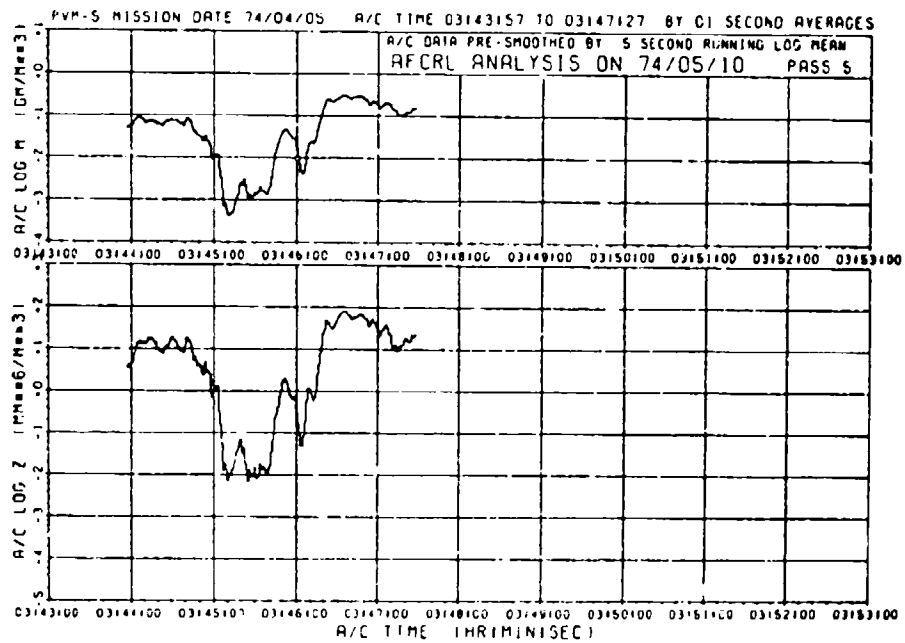


Figure 21. Water Content and Reflectivity, Computed From Aircraft Data for Pass 5 at 9.7 km

$M = 0.0191Z^{0.6314}$ $Z = 529.6 M^{1.5839}$ PASS 5 PVM-5
 PVM-5 MISSION DATE 74/04/05 A/C TIME 03:43:57 TO 03:47:27 BY 01 SECOND AVERAGES

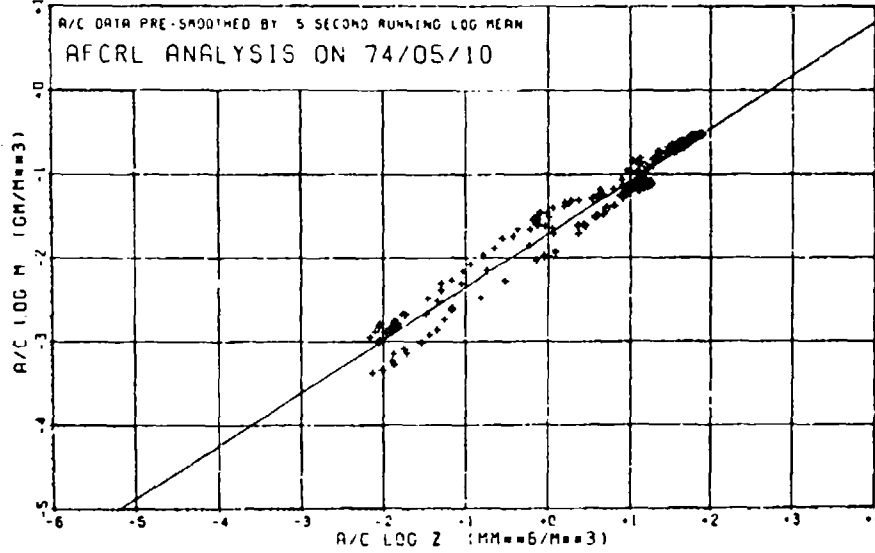


Figure 22. Correlation of M_a and Z_a Data From Figure 21

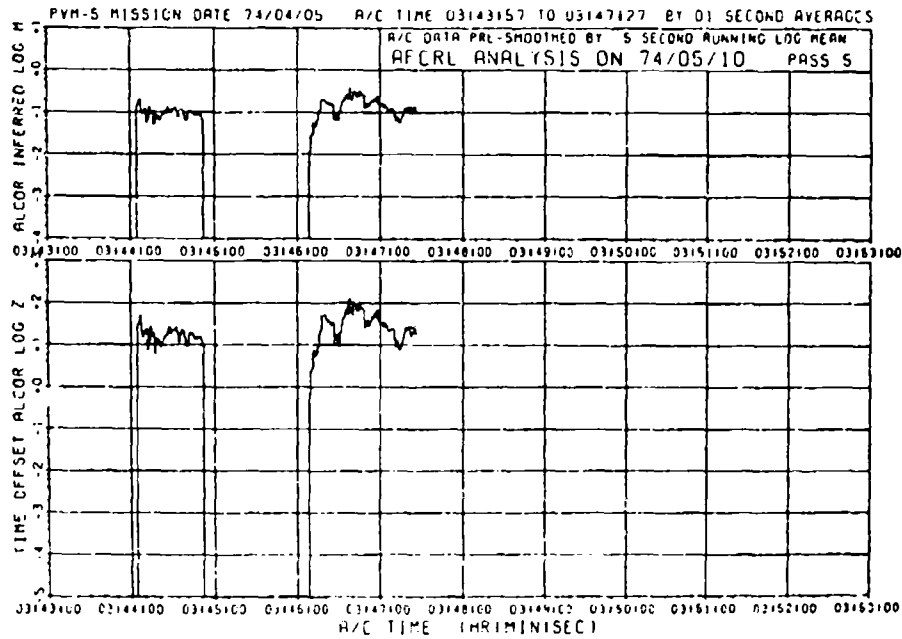


Figure 23. Reflectivity Measured by Radar (lower) and Water Content Inferred From the Reflectivity (upper) for Pass 5

$M=0.0147Z^{0.6632}$ $Z=577.0 M^{1.5078}$ PASS 5 PVM-5
 PVM-5 MISSION DATE 74/04/05 A/C TIME 03143157 TO 03147127 BY 01 SECOND PYERAGES

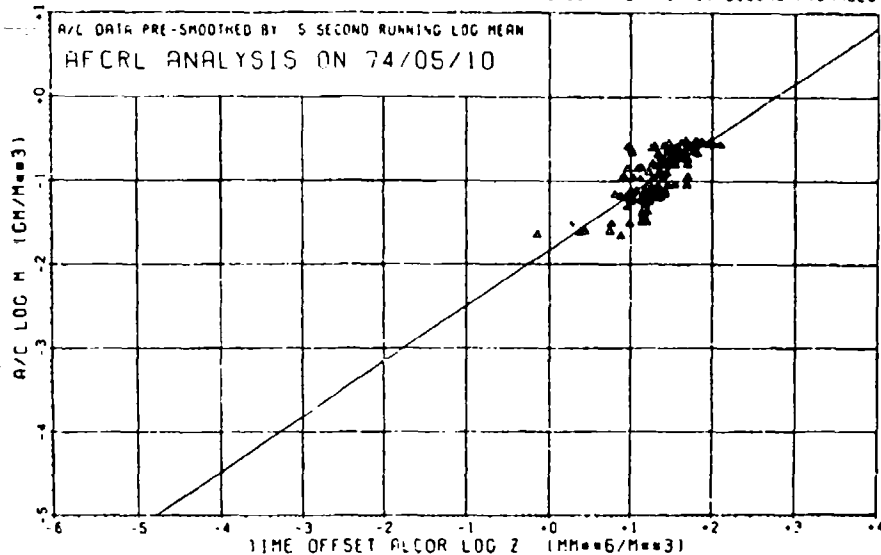


Figure 24. Correlation of M_a From Figure 21 and Z_r From Figure 23

4.6 Pass 6

This pass was flown on a 135° heading, at a mean height of 9.0 km determined by ALCOR or 27,500 ft pressure altitude. The aircraft and radar data both indicate that the clouds were primarily convective rather than stratiform. Figures 25 and 26 from the aircraft data show many points above 0.1 gm m^{-3} . Comparison of Figures 25 and 27 shows the excellent correlation between the aircraft and radar data. The correlation of Z_r and M_a over several orders of magnitude is also shown in Figure 28. Figure 28 suggests that there is an upper limit affecting the aircraft data, so that the value of M_a remains nearly constant as Z_r increases above 100 ($\log Z_r > +2$). This anomaly is due to the finite sampling length of the probe array, which does not detect all of the largest particles in the cloud. In the present case, the omission of the data points with $\log Z_r > 2$ would not change the relationship significantly.

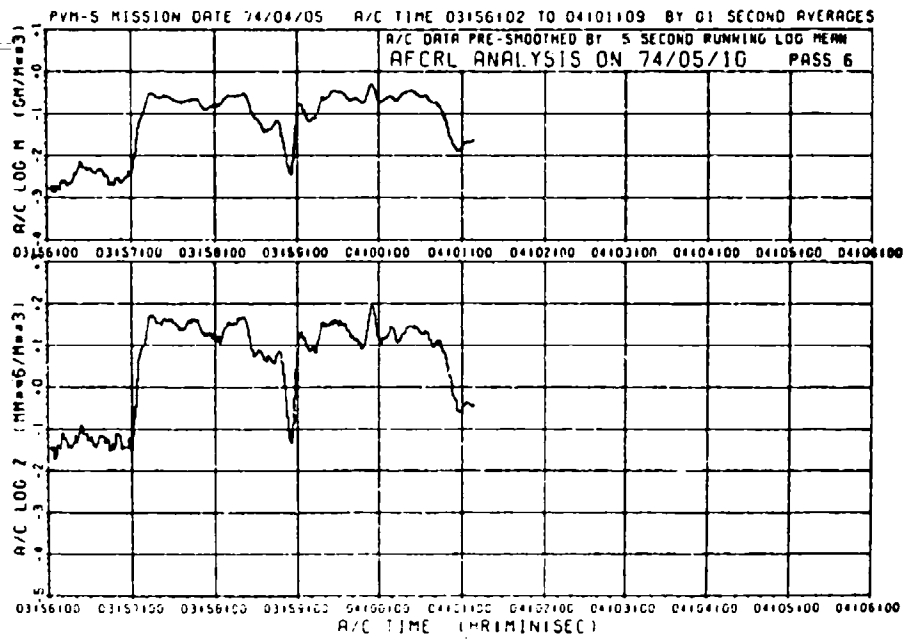


Figure 25. Water Content and Reflectivity Computed From Aircraft Data for Pass 6 at 9.0 km

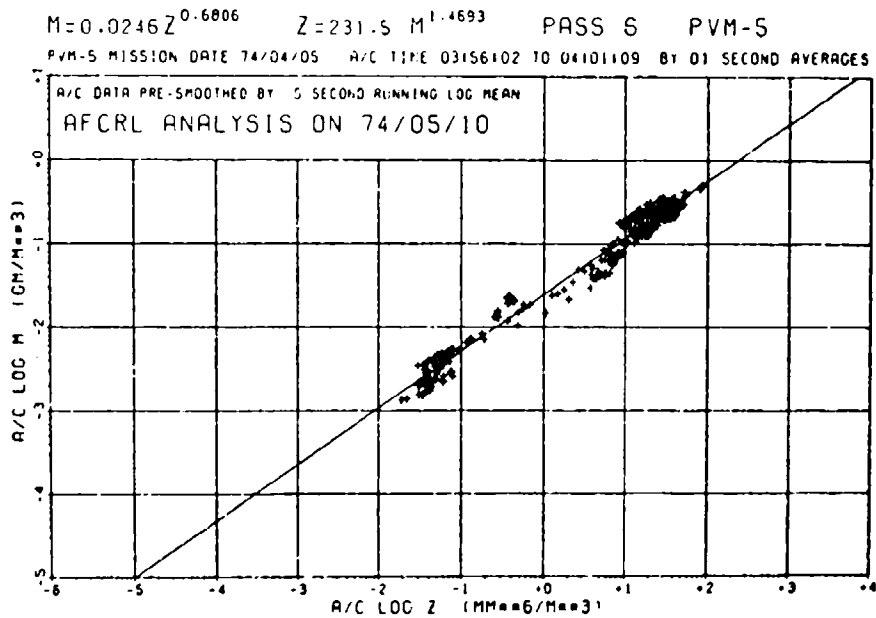


Figure 26. Correlation of M_a and Z_a Data From Figure 25

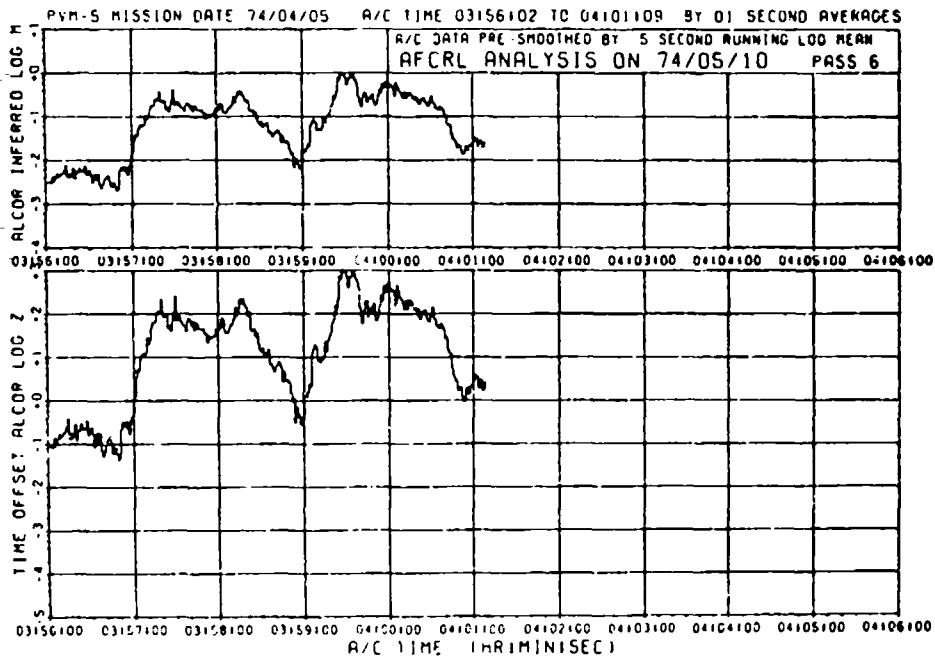


Figure 27. Reflectivity Measured by Radar (lower) and Water Content Inferred From the Reflectivity (upper) for Pass 6

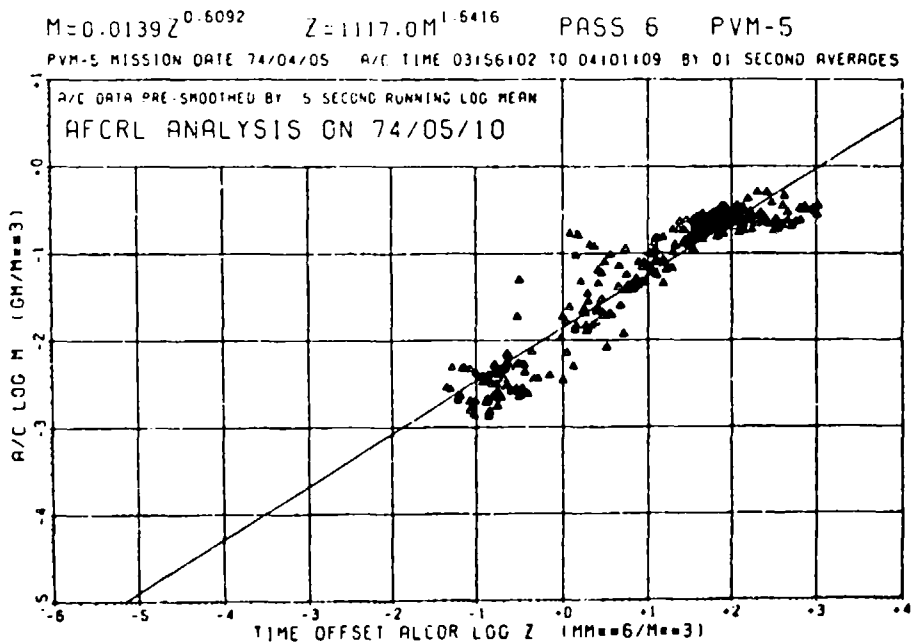


Figure 28. Correlation of M_a From Figure 25 and Z_r From Figure 27

4.7 Pass 7

This pass was on a westerly heading over Gellinam at a pressure altitude of 25,000 ft, or 8.1 km as determined by ALCOR. The clouds on this pass seemed to be more uniform than on the previous passes, as can be seen in Figures 29 and 30. Only a small amount of radar data was obtained as the transmitter was down between 0406:08 and 0409:59. Figure 31 shows the relative uniformity of the available radar data. This small amount of data and the lack of spread caused the clustering of points in Figure 32. The Z-M relation thus has very little merit and was not utilized in our subsequent analysis.

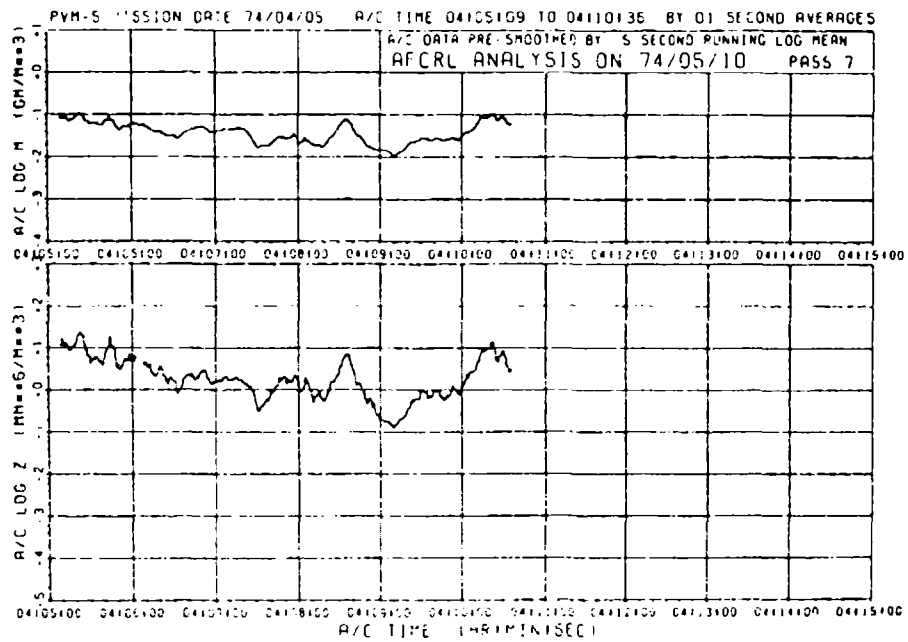


Figure 29. Water Content and Reflectivity Computed From Aircraft Data for Pass 7 at 8.1 km

$M = 0.0280Z^{0.4703}$ $Z = 2003.6M^{2.1264}$ PASS 7 PVM-5
 PVM-5 MISSION DATE 74/04/05 A/C TIME 04105109 TO 04110136 BY 01 SECOND AVERAGES

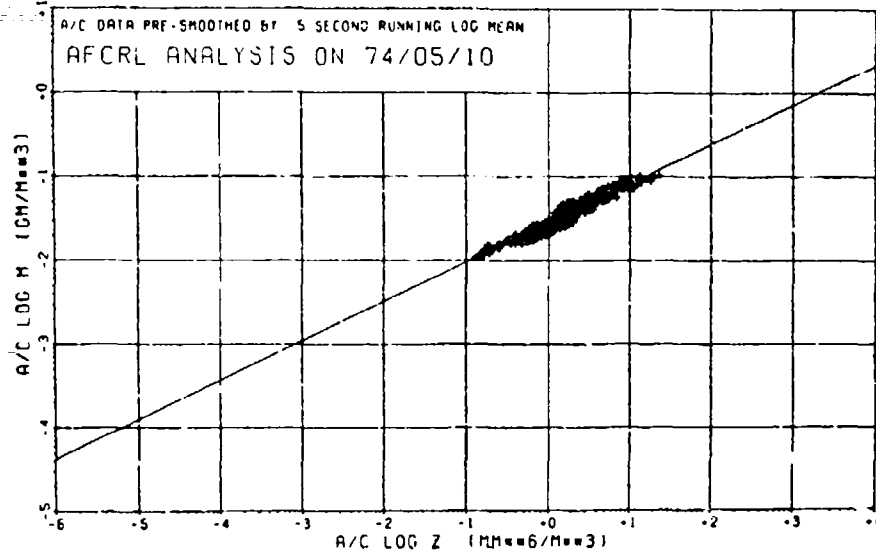


Figure 30. Correlation of M_a and Z_a Data From Figure 29

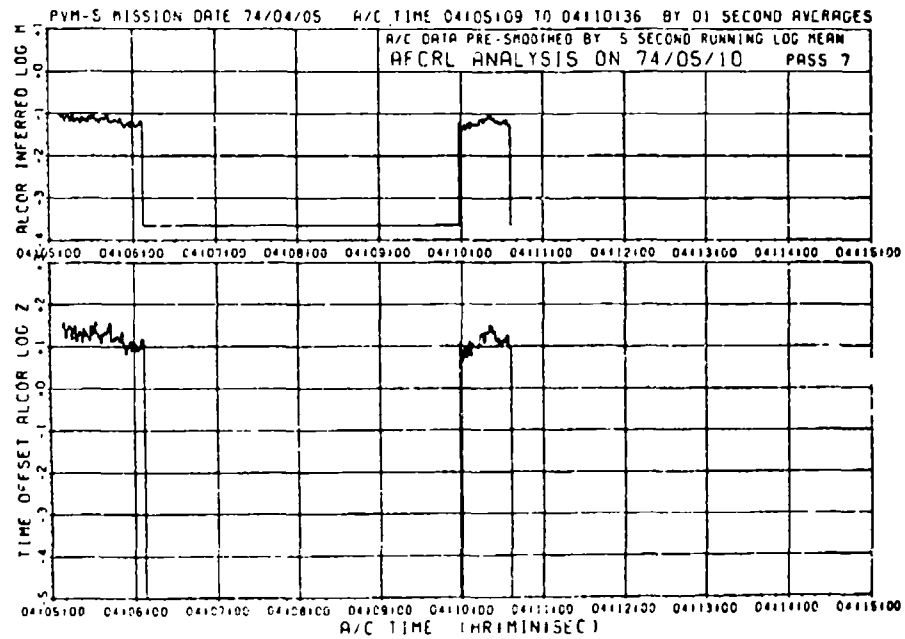


Figure 31. Reflectivity Measured by Radar (lower) and Water Content Inferred From the Reflectivity (upper) for Pass 7

$M = 0.0223 Z^{0.4002}$ $Z = 1.340 e^{+4} M^{2.4990}$ PASS 7 PVM-5
 PVM-5 MISSION DATE 74/04/05 A/C TIME 04105109 TO 04110136 BY 91 SECOND AVERAGES

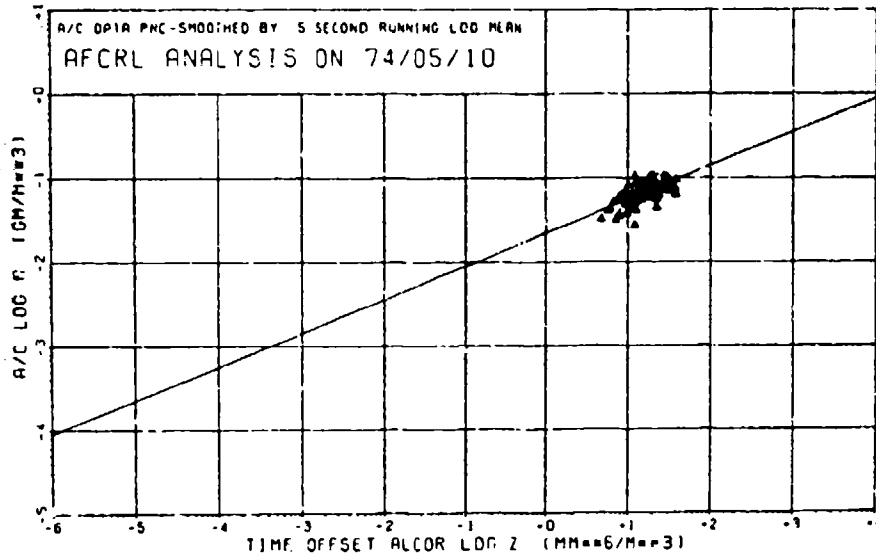


Figure 32. Correlation of M_a From Figure 29 and Z_r From Figure 31

4.8 Pass 8

The next-to-last pass was taken on a northerly heading at a radar height of 7.3 km, or 22,500 ft pressure altitude. The aircraft data in Figures 33 and 34 and the radar data in Figure 35 indicate a more stratiform situation than that found on Passes 4, 5, and 6. The omission of data at 0417:12 in Figure 35 was due to a temporary loss of the aircraft track file by ALCOR. The Z-M relation shown in Figure 36 seems reasonable, but a larger range of both Z_r and M_a would have provided better definition of the correlation for this level. This relation was used for the bottom levels because the relations from Passes 7 and 9 were unrealistic and this relation seemed compatible with the others that we used.

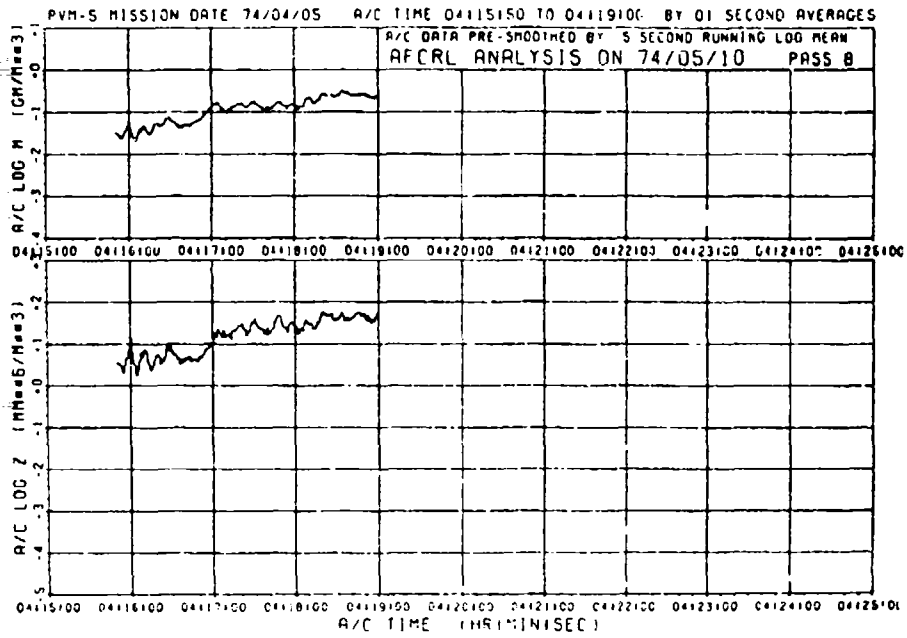


Figure 33. Water Content and Reflectivity Computed From Aircraft Data for Pass 8 at 7.3 km

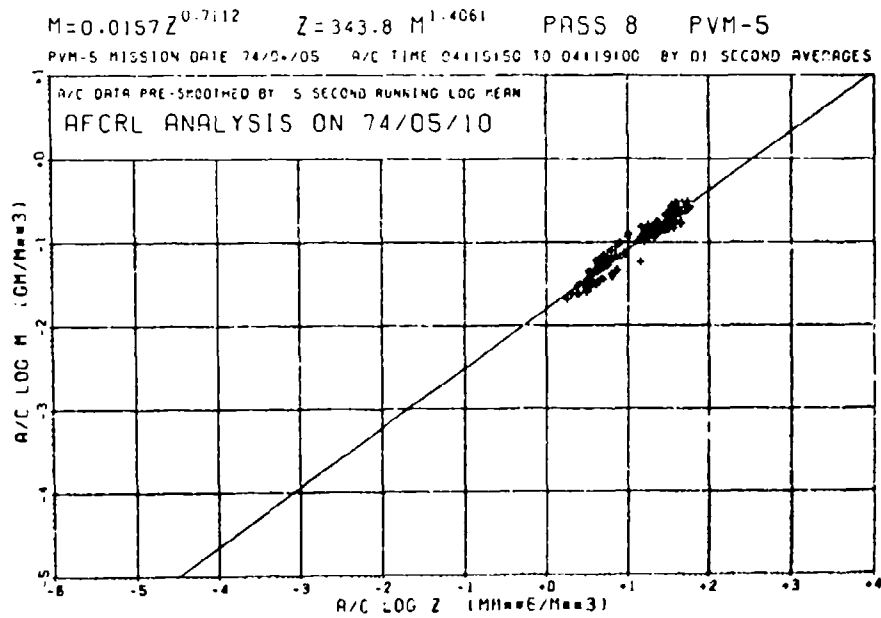


Figure 34. Correlation of M_a and Z_a Data From Figure 33

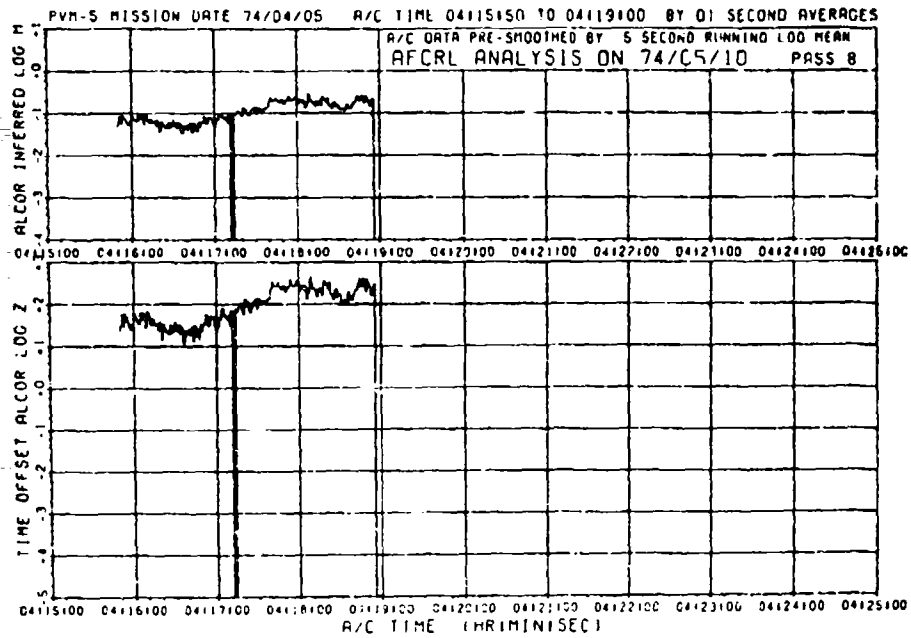


Figure 35. Reflectivity Measured by Radar (lower) and Water Content Inferred From the Reflectivity (upper) for Pass 8

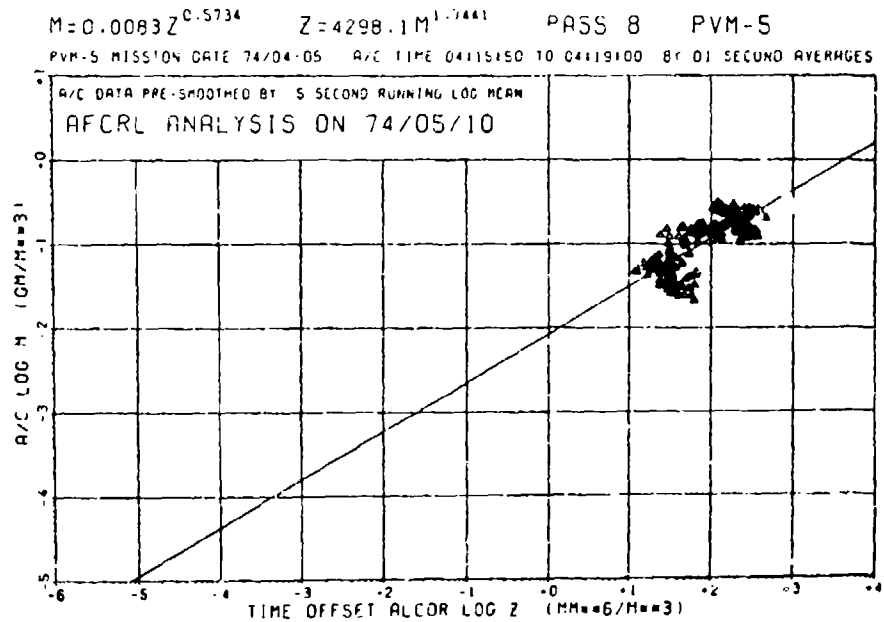


Figure 36. Correlation of M_a From Figure 33 and Z_r From Figure 35

4.9 Pass 9

The last pass was taken on a 135° heading at 6.8 km, or 20,000 ft pressure altitude. Figures 37 and 38 show that the M_a and Z_a values were substantially out of the noise. The Z_a - M_a correlation has some merit, but because of the loss of two and a half minutes of radar data (Figure 39) and because of the lack of range of both Z_r and M_a , we found it necessary to reject the Z-M relation shown in Figure 40.

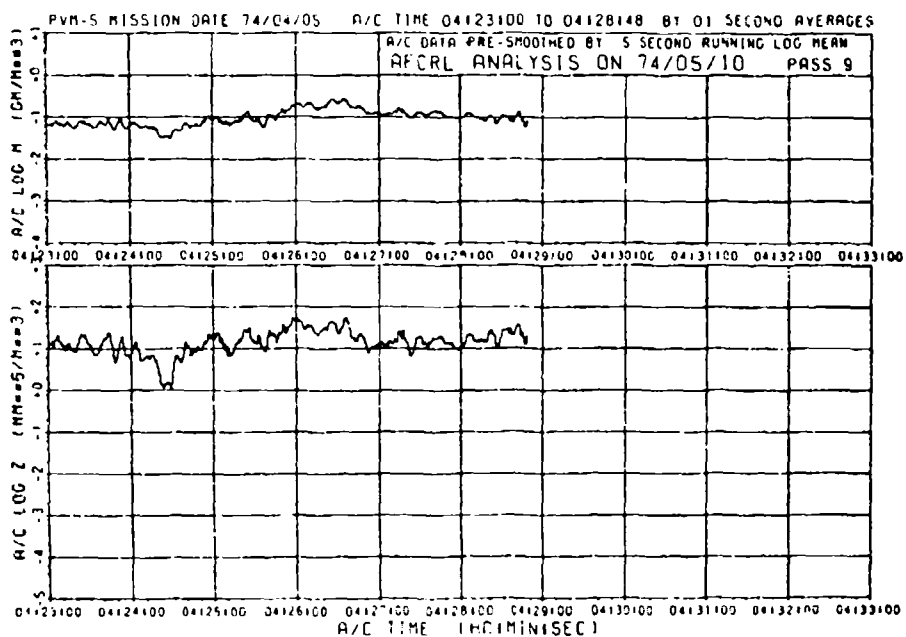


Figure 37. Water Content and Reflectivity Computed From Aircraft Data for Pass 9 at 6.6 km

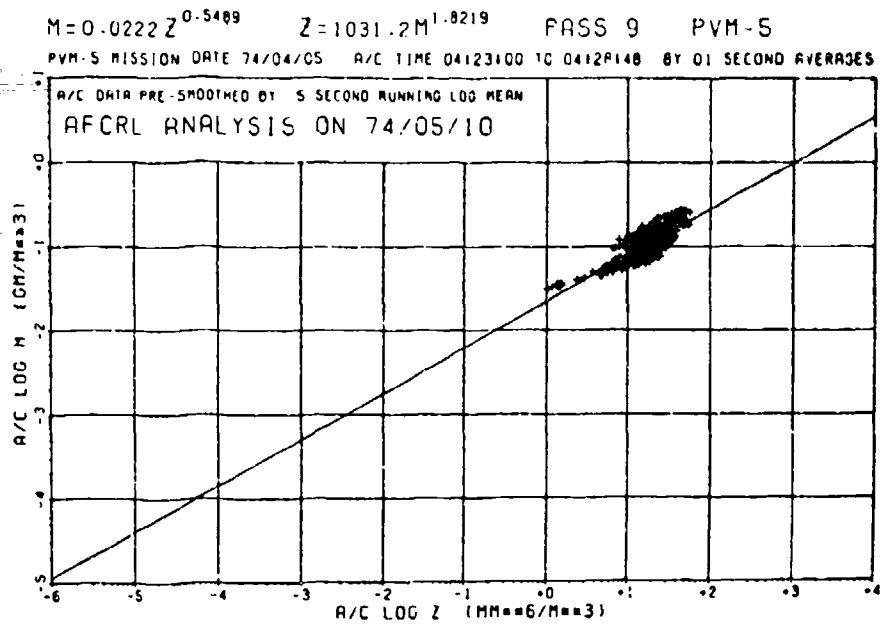


Figure 38. Correlation of M_a and Z_a Data From Figure 37

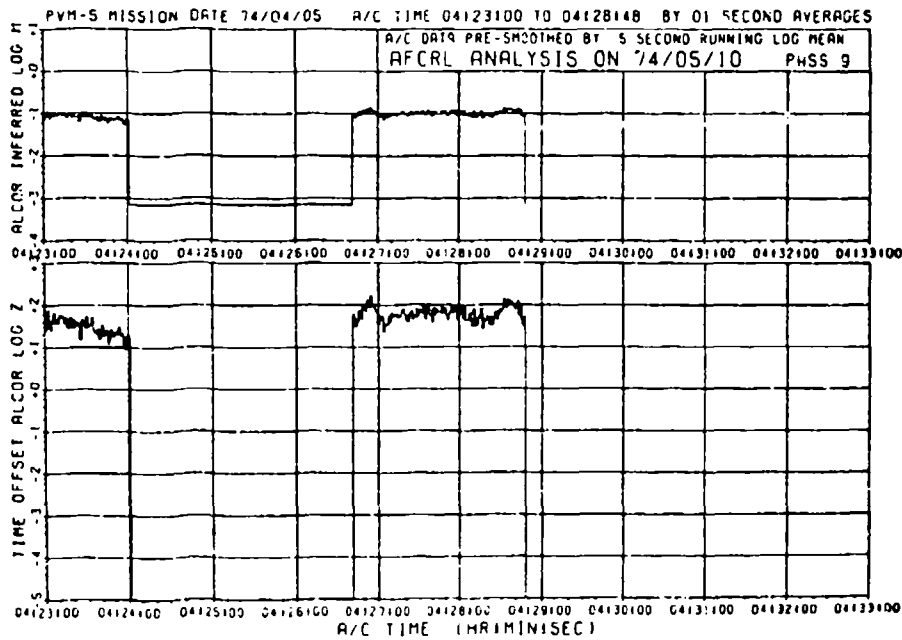


Figure 39. Reflectivity Measured by Radar (lower) and Water Content Inferred From the Reflectivity (upper) for Pass 9

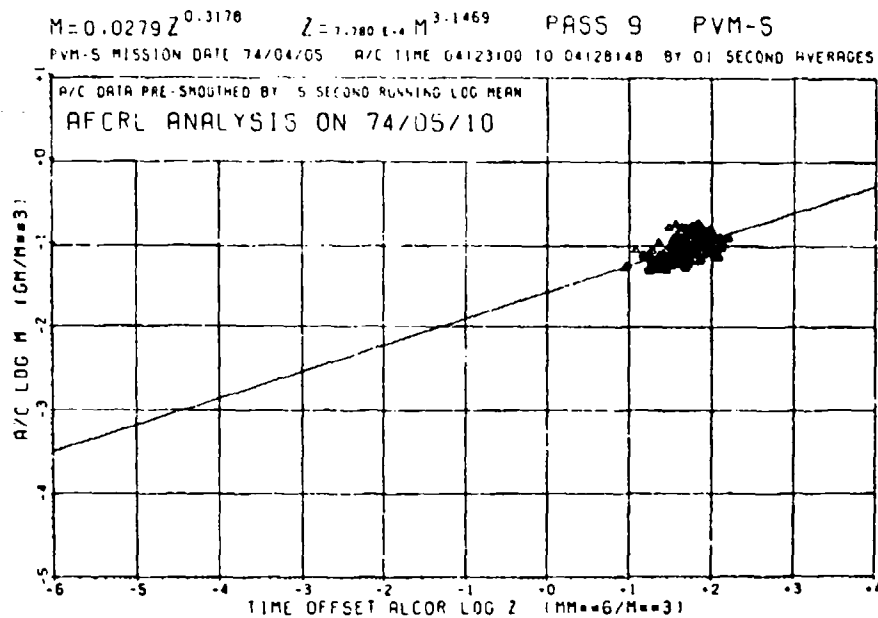


Figure 40. Correlation of M_a From Figure 37 and Z_r From Figure 39

5. INTERPRETATION OF THE RV TRAJECTORY RADAR DATA

The nine Z-M relations derived for PVM-5 mission day are shown in Figure 41, labeled by pass number, together with two standard Z-M relations for comparison. The upper dashed line shows a Z-M relation applicable to bullet and column crystals measured in mid-latitude cirrus over the U.S.⁷ This relation was used to obtain the quick-look values of ice water content and weather severity index (WSI) for the SAMSO time-urgent briefing on 16 April 1974. The lower dashed line is a Z-M relation for aggregates of plate crystals, measured at Wallops Island, Virginia. The fact that these Z-M relations bracket the correlation lines derived from the present data increases our confidence in these results. In this figure the nine Z-M relations we derived are plotted only over the ranges of the corresponding data points. The figure shows that, while the small variations of Z_r and M_a encountered on Passes 1 and 3 result in Z-M correlations which are markedly different from the others, the actual magnitudes of the numbers are generally consistent with those computed for Passes 2 and 4. Similar considerations apply to the correlations from Passes 7 and 9, where again the total

7. Heymsfield, A.J. (1973) The cirrus uncinus generating cell and the evolution of cirriform clouds, Ph. D. Thesis, The University of Chicago.

range of Z_r and M_a was quite small. Of the remaining passes, all are fairly close together except Pass 8, which is parallel to the other relations but gives lower water content values for the same Z_r values. As noted in the discussion of Pass 8, the clouds seemed to be more stratiform on this pass, while the clouds were more convective on Passes 2, 4, 5, and 6. Radar theory and observations indicate that when snow crystals begin to aggregate the Z values increase for the same values of M . If aggregation were occurring on Pass 8, one would expect the Z - M relation to be moved to the right of the others in Figure 41, as is seen.

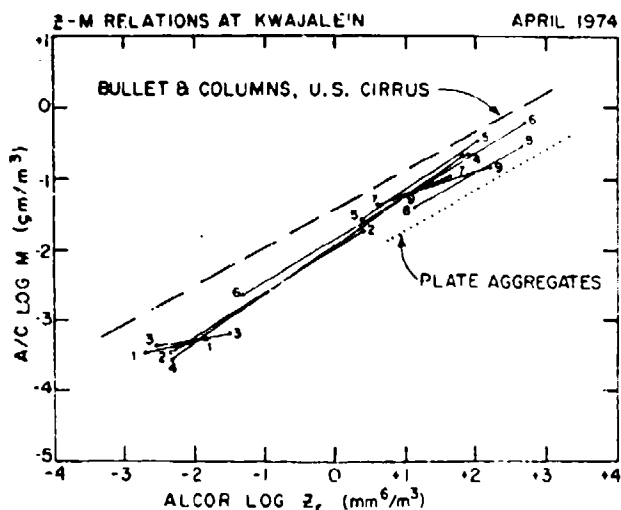


Figure 41. Composite of Z - M Equations Derived From PVM-5 Correlation Data. Equations appropriate to bullet and column crystals, measured in Continental U.S. cirrus, and plate aggregates, measured at Wallops Island, Va., are shown for comparison

The parameters of the derived Z - M relations are listed in Table 1. The values of the exponents for the equations of Passes 1, 3, 7, and 9 are distinctly less than those for the other passes. We used the Z - M relations from Passes 2, 4, 5, 6, and 8 to interpret the values of Z_r measured by ALCOR along the RV trajectories following the mission. Each was initially applied to the height increment between the next adjacent measurements above and below, with that from Pass 2 applied from the top of the scan to the height of Pass 4, and that from Pass 8 applied from the height of Pass 6 to the bottom of the scan. These height increments are also listed in Table 1.

Table 1. $Z_r - M_a$ Relations, April 1974

Pass Number	Height (km)	$M_a \text{ (gm m}^{-3}\text{)} = A Z_r \text{ (mm}^6 \text{ m}^{-3}\text{)}^B$		Range of Applicability (km)
		Coefficient (A)	Exponent (B)	
1	12.9	0.0017	0.2594	NOT USED
2	12.1	0.0106	0.6334	Above 10.4
3	11.4	0.0010	0.1596	NOT USED
4	10.4	0.0114	0.6878	9.7 - 12.1
5	9.7	0.0147	0.6632	9.0 - 10.4
6	9.0	0.0139	0.6092	7.3 - 9.7
7	8.1	0.0223	0.4002	NOT USED
8	7.3	0.0083	0.5734	Below 9.0
9	6.6	0.0279	0.3178	NOT USED

The resulting values of M_r , that is, M computed from Z_r , were interpolated between flight levels so that each Z - M relation was applied exactly at the height of its measurement, with a smooth transition from one relation to the next. The resulting profiles of M_r are shown in Figures 42, 43, and 44, for RV's 1, 2, and 3, respectively. The first post-impact scan of each trajectory, interpreted in the manner just described, is shown in each of these figures. Profiles of M_r previously computed using the "bullets and columns" Z - M equation are shown in Figures 42, 43 and 44 for comparison. Figure 41 shows that this earlier approximation yields higher values of M_r than the equations we derived from the PVM-5 correlation data by a factor of 1.6 (2 dB) to 6.3 (8 dB). The values of WSI computed for the layers in which the radar returns were above noise, that is, the layers in which the M_r profiles are drawn, are given for each computed M_r profile.

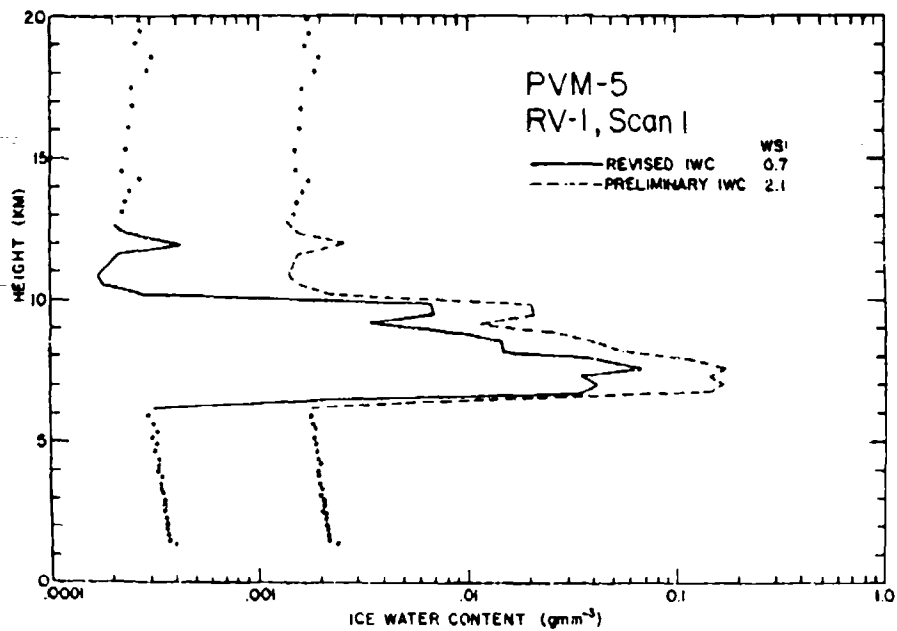


Figure 42. Water Content Profile on PVM-5, RV 1 Trajectory. Preliminary estimate was based on "bullet and column" Z-M equation (Figure 41) and was high by a factor of about 3

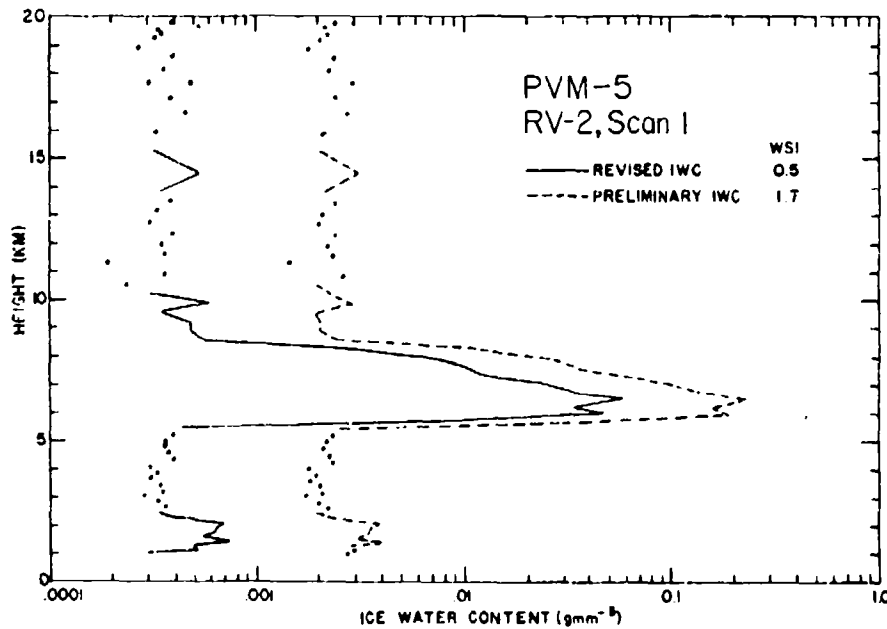


Figure 43. Water Content Profile on PVM-5, RV 2 Trajectory. Preliminary estimate was based on "bullet and column" Z-M equation (Figure 41) and was high by a factor of about 3

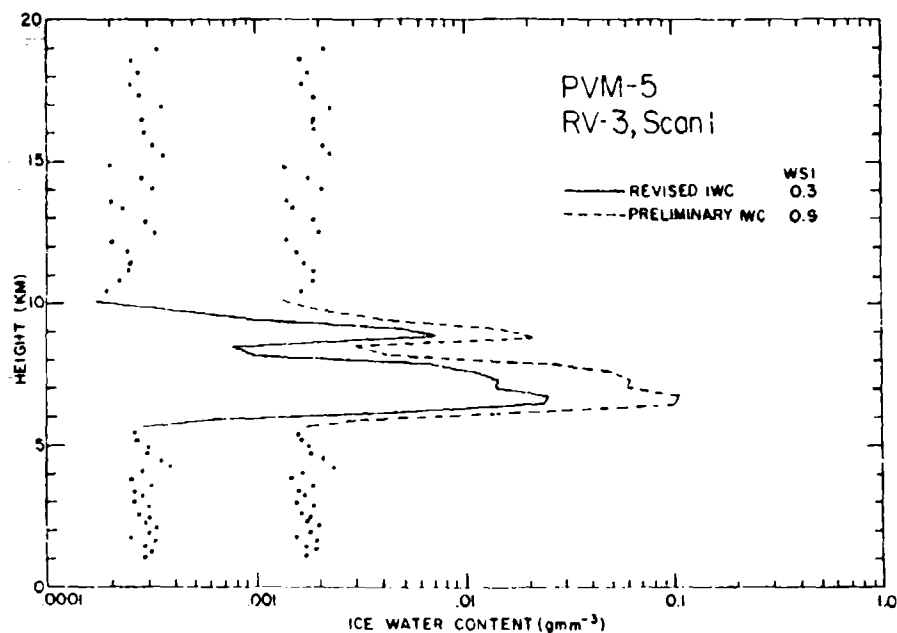


Figure 44. Water Content Profiles on PVM-5, RV 3 Trajectory. Preliminary estimate was based on "bullet and column" Z-M equation (Figure 41) and was high by a factor of about 3

6. CONCLUSIONS

The quantitative reliability of the ice water content analysis is primarily dependent on the reliability of the M values obtained from the aircraft data and supplied to AFCRL by MRI. This involves the selection of crystal habit from the replicator films by MRI, and the uncertainties noted above due to the missing cloud probe data and the apparent high-M cutoff of the PMS probes. The absence of the cloud probe data tends to decrease the values of M at the lower end of the curves. The upper limit on the M values obtained by the aircraft, noted in the discussion of Figure 28, has also been observed in PMS data taken at Wallops Island and is currently under investigation.

An independent check on the validity of the aircraft data could be obtained by comparing the values of Z_a derived from the aircraft data and Z_r measured by the radar. Such a comparison requires that Z_r be known accurately. For this purpose we conducted an experiment with the TTR-4 radar in December 1973 involving weather observations in chirp and constant-frequency mode. Results of the analysis of these data will be presented in a future report. Our preliminary estimate of the absolute accuracy of the ALCOR Z_r is 6 dB, or a factor of 4. We

emphasize, however, that with the analysis technique described in this report, any error in Z_r drops out in the computation of M_r on the trajectories.

All of the data points taken during the correlation passes fell within reasonable upper and lower bounds on the Z-M plots. The Z-M line for bullet and column crystals, which is slightly high for these data, is essentially an upper bound. The lower bound is the curve for aggregates of plate crystals. From the available data, we feel that the values of M and WSI derived for the trajectories are essentially correct. We also feel that any corrections applied to account for the absence of the cloud probe or the high-M cutoff of the PMS probes will not change the M values by more than 2 or 3 dB (a factor of 2).

The link-offset mode of obtaining the correlation data proved to be quite good, from both the operational and the data-reduction points of view. It is possible to obtain the radar data as little as 30 sec prior to the aircraft sampling of a given point, and the resulting series of values of M_a and Z_r are fairly easy to handle in the computer.

References

1. Plank, V. G. (1974a) A summary of the radar equations and measurement techniques used in the SAMS rain erosion program at Wallops Island, Virginia. AFCRL-TR-0053, Air Force Cambridge Research Laboratories, Hanscom AFB, Mass.
2. Plank, V. G. (1974b) Hydrometeor parameters determined from the radar data of the SAMS rain erosion program. AFCRL-TR-74-0249, Air Force Cambridge Research Laboratories, Hanscom AFB, Mass.
3. Plank, V. G. (1974c) Liquid-water content and hydrometeor size-distribution information for the SAMS missile flights of the 1971-1972 season at Wallops Island, Virginia. AFCRL-TR-74-0296, Air Force Cambridge Research Laboratories, Hanscom AFB, Mass.
4. Barnes, A. A., Jr., Nelson, L. D., and Metcalf, J. I. (1974) Weather Documentation at Kwajalein Missile Range. 6th Conf. Aerosp. and Aeronaut. Meteor., Amer. Meteor. Soc. pp 66-69; AFCRL-TR-74-0430, Air Force Cambridge Research Laboratories, Hanscom AFB, Mass.
5. Knollenberg, R. G. (1970) The optical array: An alternative to scattering or extinction for airborne particle size determination, J. Appl. Meteor. 9:96-103.
6. Heymsfield, A. J., and Knollenberg, R. G. (1972) Properties of cirrus generating cells, J. Atmos. Sci. 29:1358-1366.
7. Heymsfield, A. J. (1973) The cirrus uncinus generating cell and the evolution of cirriform clouds, Ph. D. Thesis, The University of Chicago.

Symbols

ABRES	Advanced Ballistic Re-Entry Systems
AFCRL	Air Force Cambridge Research Laboratories
ALCOR	ARPA-Lincoln C-band Observables Radar
ARPA	Advanced Research Projects Agency
KMR	Kwajalein Missile Range
KREMS	Kiernan Re-Entry Measurements Site
LIDAR	Light Detection and Ranging (optical analog of RADAR)
M	Water content (liquid or ice), gm m^{-3}
MRI	Meteorology Research, Inc., Altadena, Calif.
PMS	Particle Measuring Systems, Inc., Boulder, Colo.
PRESS	Pacific Range Electromagnetic Signature Studies
PRF	Pulse Repetition Frequency
PVM	Production Verification Missile
RV	Re-Entry Vehicle
SAMSO	Space and Missile Systems Organization
WSI	Weather Severity Index (height-weighted integrated water content)
Z	Radar reflectivity factor, $\text{mm}^6 \text{m}^{-3}$